Electronic Supplementary Information for

Quinodimethane embedded expanded helicenes and their open-shell diradical dications/dianions

Qing Jiang, Yi Han, Ya Zou & Chunyan Chi*

Department of Chemistry, National University of Singapore, 3 Science Drive 3, 117543, Singapore

Email: chmcc@nus.edu.sg

Table of Contents

1. Experimental Section

1.1 General

All reagents were purchased from commercial sources without further pur ification. Anhydrous dichloromethane (DCM) was distilled from CaH_2. Anhydrous THF was distilled from sodium-benzophenone immediately prior to use. ^1H and ^{13}C NMR spectra were recorded using 500 MHz Bruker spectrometer in $CDCl_3$, CD_2Cl_2, CD_3CN, or THF-d_8 with tetramethylsilane (TMS) as the internal standard. The chemical shift was recorded in ppm and the following abbreviations were used to explain the multiplicities: s = singlet, d = doublet, t = triplet, m = multiplet, br = broad. HR APCI mass spectra were recorded on a MicrOTOFQII instrument. UV-vis absorption was recorded on a Shimadzu UV-3600 spectrophotometer. Cyclic voltammetry measurements were performed in dry dichloromethane on a CHI 620C electrochemical analyzer with a three-electrode cell, using 0.1 M Bu_4NPF_6 as supporting electrolyte, AgCl/Ag as reference electrode, gold disk as working electrode, Pt wire as counter electrode, and scan rate at 100 mV s^{-1}. The potential was externally calibrated against the ferrocene/ferrocenium couple. The single crystal was measured at low temperature (T = 100K) on a four circles goniometer Kappa geometry Bruker AXS D8 Venture equipped with a Photon 100 CMOS active pixel sensor detector using a Copper monochromatized (= 1.54178 Å) X-Ray radiation. Continuous wave X-band ESR spectra were obtained with a Bruker ELEXSYS E500 spectrometer using a variable temperature Bruker liquid nitrogen cryostat.

1.2. Synthetic procedures and characterization data
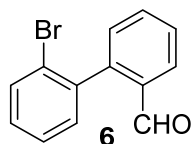
A mixture of THF (25 mL) and H_2O (5 mL) was sparged with N_2. After 20 min, **3** (1.84 g, 10 mmol), **5** (2.4 g, 12 mmol), K_2CO_3 (2.76 g, 20 mmol) and Pd(PPh$_3$)$_4$ (300 mg, 0.26 mmol) were added to the flask. The reaction mixture was heated at 90 °C for 24 h under nitrogen. After cooling to room temperature, the resulting suspension was filtered and washed with diethyl ether. The combined filtrates were concentrated under reduced pressure and purified on a silica-gel column chromatography (hexane/CH$_2$Cl$_2$ = 3:1, v/v) to give 2.44 g of compound **6** in 94% yield as a colorless solid. ^1H NMR (CDCl$_3$, 500 MHz): δ ppm 9.80 (s, 1H), 8.04 (dd, ^3J = 7.8 Hz, ^4J = 1.2 Hz, 1H), 7.69 (dd, ^3J = 8.0 Hz, ^4J = 1.3 Hz, 1H), 7.66 (td, ^3J = 7.5 Hz, ^4J = 1.5 Hz, 1H), 7.54 (tt, ^3J = 7.5 Hz, ^4J = 1.1 Hz, 1H), 7.41 (td, ^3J = 7.5 Hz, ^4J = 1.3 Hz, 1H), 7.33-7.28 (m, 3H); ^{13}C NMR (CDCl$_3$, 125 MHz) δ ppm 191.6, 144.6, 139.0, 133.8, 133.7, 132.9, 131.7, 131.0, 130.0, 128.7, 127.6, 127.5, 124.0; HR-MS (APCI): calcd for C$_{13}$H$_9$BrO (M+H)$^+$: 260.9837; found, 260.9838 (error: 0.38 ppm).

7
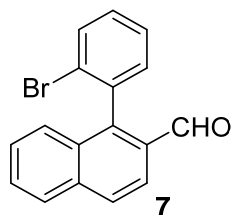
A mixture of THF (25 mL) and H_2O (5 mL) was sparged with N_2. After 20 min, **4** (2.34 g, 10 mmol), **5** (2.4 mg, 12 mmol), K_2CO_3 (2.76 g, 20 mmol) and $Pd(PPh_3)_4$ (300 mg, 0.26 mmol) were added to the flask. The reaction mixture was heated at 90 °C for 24 h under nitrogen. After cooling to room temperature, the resulting suspension was filtered and washed with diethyl ether. The combined filtrates were concentrated under reduced pressure and purified on a silica-gel column chromatography (hexane/CH_2Cl_2 = 3:1, v/v) to give 3.04 g of compound **7** in 98% yield as a colorless solid. ^1H NMR (CDCl$_3$, 500 MHz): δ ppm 9.83 (s, 1H), 8.08 (d, J = 8.65 Hz, 1H), 7.99 (d, J = 8.6 Hz, 1H), 7.95 (d, J = 8.15 Hz, 1H), 7.79 (d, J = 8.0 Hz, 1H), 7.63 (td, ^3J = 7.1 Hz, ^4J = 1.6 Hz, 1H), 7.51-7.44 (m, 3H), 7.33 (td, ^3J = 7.7 Hz, ^4J = 1.7 Hz, 1H), 7.38 (dd, ^3J = 7.4 Hz, ^4J = 1.7 Hz, 1H); ^{13}C NMR (CDCl$_3$, 125 MHz) δ ppm 192.1, 145.2, 136.7, 136.4, 133.1, 132.7, 132.0 ,131.2, 130.4, 129.2, 129.1, 128.6, 127.5, 127.4, 127.2, 125.1, 122.3; HR-MS (APCI): calcd for $C_{17}H_{12}BrO$ (M+H)$^+$: 311.0027; found, 311.0026 (error: -0.52 ppm).
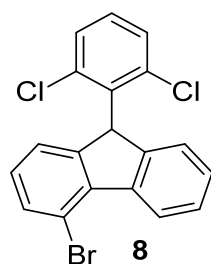
8

To an oven dried flask was added THF (150 mL) and 2.6-dichloro-1-bromobenzene (3.36 g, 15 mmol). The mixture was cooled to 0 °C and isopropylmagnesium chloride (2.0 M, 7 mL) was added slowly. The reaction was stirred for 2 h and then the compound **6** (2.34 g, 9 mmol) was added quickly in one portion. The mixture was warmed to room temperature overnight. The reaction was quenched with saturated NH_4Cl solution and the organic phase was washed with water and then brine solution. The organic layer was dried over Na_2SO_4 and the volatiles removed. The crude product was then dissolved in 100 mL dry DCM under nitrogen atmosphere and 2 mL of $BF_3 \cdot OEt_2$ was added. The mixture was stirred for 30 minutes and quenched by methanol. The solvent was removed under reduced pressure and the residue was purified by column chromatography (hexane:DCM = 5:1, v/v) to give compound **8** (86%, 3.0 g) as a colorless solid. ^1H NMR (500 MHz, CDCl$_3$): δ (ppm) 8.68 (d, J = 7.85 Hz, 1H), 7.58 (d, J = 7.9 Hz, 1H), 7.52 (dd, ^3J = 8.0 Hz, ^4J = 1.3 Hz, 1H), 7.48 (t, J = 7.6 Hz, 1H), 7.35 (td, ^3J = 7.5 Hz, ^4J = 0.7 Hz, 1H), 7.26-7.23 (m, 1H), 7.21-7.17 (m, 2H), 7.14-7.10 (m, 2H), 6.01 (s, 1H); ^{13}C NMR (125 MHz, CDCl$_3$): δ (ppm) 148.2, 145.7, 141.0, 139.9, 137.5, 136.1, 136.0, 132.4, 130.1, 129.2, 128.3, 128.1, 128.0, 127.2, 123.8, 123.7, 122.8, 117.3, 50.7; HR-MS analysis (APCI): calcd for $C_{19}H_{11}BrCl_2$ (M+H)$^+$: 388.9421; found, 388.9423 (error: 0.52 ppm).
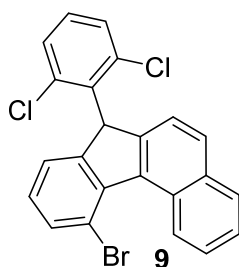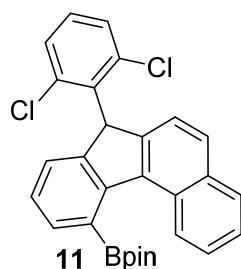
To an oven dried flask was added THF (150 mL) and 2,6-dichloro-1-bromobenzene (3.36g, 15 mmol). The mixture was cooled to 0 °C and isopropylmagnesium chloride (2.0 M, 7 mL) was added slowly. The reaction was stirred for 2 h and then the compound **7** (2.79 g, 9 mmol) was added quickly in one portion. The mixture was warmed to room temperature overnight. The reaction was quenched with saturated NH_4Cl solution and the organic phase was washed with water and then brine solution. The organic layer was dried over Na_2SO_4 and the volatiles removed. The crude product was then dissolved in 100 mL dry DCM under nitrogen atmosphere and 2 mL of $BF_3 \cdot OEt_2$ was added. The mixture was stirred for 30 minutes and quenched by methanol. The solvent was removed under reduced pressure and the residue was purified by column chromatography (hexane:DCM = 5:1, v/v) to give compound **9** (84%, 3.31 g) as a colorless solid. ^1H NMR (500 MHz, $CDCl_3$): δ (ppm) 9.18 (d, J = 8.6 Hz, 1H), 7.92 (d, J = 8.0 Hz, 1H), 7.86 (d, J = 8.2 Hz, 1H), 7.74 (d, J = 7.85 Hz, 1H), 7.61 (td, ^3J = 8.2 Hz, ^4J = 1.4 Hz, 1H), 7.55-7.51 (m, 2H), 7.31 (d, J = 8.2 Hz, 1H), 7.23 (dt, ^3J = 7.3 Hz, ^4J = 1.2 Hz, 1H), 7.20 (t, J = 8.1 Hz, 1H), 7.15 (t, J = 7.65 Hz, 1H), 7.11 (dd, ^3J = 8.0 Hz, ^4J = 1.2 Hz, 1H), 6.07 (s, 1H); ^{13}C NMR (125 MHz, $CDCl_3$): δ (ppm) 149.4, 145.1, 142.7, 137.8, 136.1, 135.7, 134.4, 134.1, 130.2, 130.1, 129.3, 129.1, 128.7, 128.4, 127.8, 125.5, 124.9, 122.6, 121.4, 116.4, 51.7; HR-MS analysis (APCI): calcd for $C_{23}H_{13}BrCl_2$ $(M+H)^+$: 438.9656; found, 438.9659 (error: 0.68 ppm).
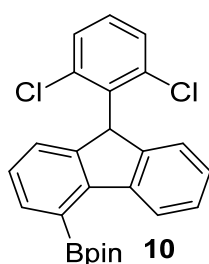

To an oven dried flask was added **8** (2.8 g, 7.2 mmol), $B(pin)_2$ (3.24 g, 14.4 mmol), $Pd(dppf)Cl_2$ (527 mg, 0.72 mmol), KOAc (2.98 g, 21.6 mmol) and dioxane (20 mL). The reaction mixture was heated at 90 °C for 15 h under nitrogen. After cooling to room temperature, the resulting suspension was filtered and washed with diethyl ether. The combined filtrates were concentrated under reduced pressure and purified on a silica-gel column chromatography (hexane/CH_2Cl_2 = 2:1, v/v) to give 2.26 g of compound **10** in 72% yield as a colorless solid. ^1H NMR ($CDCl_3$, 500 MHz): δ ppm 8.81 (d, J = 7.85 Hz, 1H), 7.89 (d, J = 7.15 Hz, 1H), 7.52 (dd, ^3J = 8.0 Hz, ^4J = 1.2 Hz, 1H), 7.43 (t, J = 7.6 Hz, 1H), 7.32-7.27 (m, 3H), 7.22 (d, J = 7.35 Hz, 1H), 7.18 (t, J = 7.95 Hz, 1H), 7.12 (dd, ^3J = 8.0 Hz, ^4J = 1.1 Hz, 1H), 5.95 (s, 1H), 1.51 (s, 6H), 1.49 (s, 6H); ^{13}C NMR ($CDCl_3$, 125 MHz) δ ppm 146.3, 145.9, 145.7, 142.9, 137.6, 136.9, 136.0, 135.5, 130.1, 128.8, 128.2, 127.2, 126.4, 126.2, 124.3, 123.6, 84.3, 50.5, 25.2; HR-MS (APCI): caldc for $C_{25}H_{23}BCl_2O_2$ $(M+H)^+$: 437.1168; found,

437.1165 (error: -0.69 ppm).

11 Bpin

To an oven dried flask was added **9** (3 g, 6.8 mmol), B(pin)$_2$ (3.45 g, 13.6 mmol), Pd(dppf)Cl$_2$ (498 mg, 0,68 mmol), KOAc (2g, 20.4 mmol) and dioxane (20 mL). The reaction mixture was heated at 90 $^{\circ}$C for 15 h under nitrogen. After cooling to room temperature, the resulting suspension was filtered and washed with diethyl ether. The combined filtrates were concentrated under reduced pressure and purified on a silica-gel column chromatography (hexane/CH$_2$Cl$_2$ = 2:1, v/v) to give 2.16 g of compound **11** in 65% yield as a colorless solid. ^{1}H NMR (CDCl$_3$, 500 MHz): δ ppm 8.50 (d, J = 8.3 Hz, 1H), 7.92 (d, J = 8.0 Hz, 1H), 7.79 (t, J = 6.6 Hz, 2H), 7.57-7.51 (m, 2H), 7.49 (t, J = 7.4 Hz, 1H), 7.35-7.32 (m, 2H), 7.30 (t, J = 7.3 Hz, 1H), 7.17 (t, J = 8.0 Hz, 1H), 7.07 (dd, ^3J = 8.0 Hz, ^4J = 1.1 Hz, 1H), 6.02 (s, 1H), 1.42 (s, 6H), 1.39 (s, 6H); ^{13}C NMR (CDCl$_3$, 125 MHz) δ ppm 146.9, 145.2, 144.3, 138.5, 137.8, 136.3, 136.2, 133.9, 133.6, 130.1, 129.4, 128.9, 128.7, 128.2, 126.2, 125.7, 125.6, 125.3, 125.2, 122.0, 84.4, 51.3, 25.4; HR-MS (APCI): caldc for C$_{29}$H$_{25}$BCl$_2$O$_2$ (M+H)$^+$: 487.1403; found, 487.1405 (error: 0.52 ppm).

13
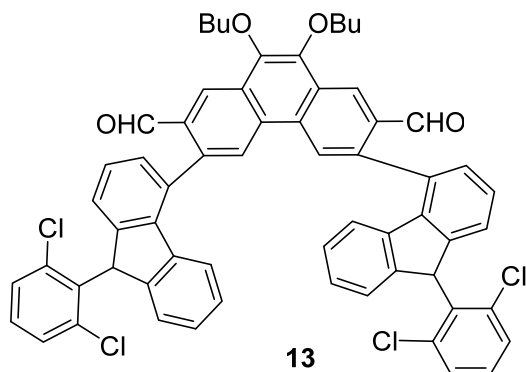
A mixture of THF (15 mL) and H$_2$O (3 mL) was sparged with N$_2$. After 20 min, **10** (654 mg, 1.5 mmol), **12** (268 mg, 0.5 mmol), K$_2$CO$_3$ (0.35 g, 2.5 mmol) and Pd(PPh$_3$)$_4$ (200 mg, 0.17 mmol) were added to the flask. The reaction mixture was heated at 90 $^{\circ}$C for 48 h under nitrogen. After cooling to room temperature, the resulting suspension was filtered and washed with diethyl ether. The combined filtrates were concentrated under reduced pressure and purified on a silica-gel column chromatography (hexane/CH$_2$Cl$_2$ = 1:1, v/v) to give 457 mg of **13** in 92% yield as a yellow solid. The structural characterization of **13** with NMR spectroscopy is not possible due to the presence of a mixture of non-isolable stereoisomers resulting in a very complex NMR spectrum (Figures S34 and 35). HR-MS (APCI): caldc for C$_{62}$H$_{46}$Cl$_4$O$_4$ (M+H)$^+$: 995.2150; found, 995.2153 (error: 0.3 ppm).

14
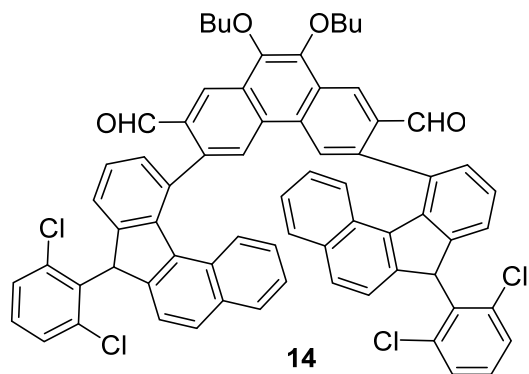
A mixture of THF (15 mL) and H_2O (3 mL) was sparged with N_2. After 20 min, **11** (0.73 g, 1.5 mmol), **12** (268 mg, 0.5 mmol), K_2CO_3 (0.35 g, 2.5 mmol) and $Pd(PPh_3)_4$ (200 mg, 0.17 mmol) were added to the flask. The reaction mixture was heated at 90 °C for 48 h under nitrogen. After cooling to room temperature, the resulting suspension was filtered and washed with diethyl ether. The combined filtrates were concentrated under reduced pressure and purified on a silica-gel column chromatography (hexane/CH_2Cl_2 = 1:1, v/v) to give 470 mg of **14** in 86% yield as a yellow solid. The structural characterization of **14** with NMR spectroscopy is not possible due to the presence of a mixture of non-isolable stereoisomers resulting in a very complex NMR spectrum (Figures S36 and 37). HR-MS (APCI): caldc for $C_{70}H_{50}Cl_4O_4$ (M+H)$^+$: 1095.2463; found, 1095.2465 (error: 0.18 ppm).
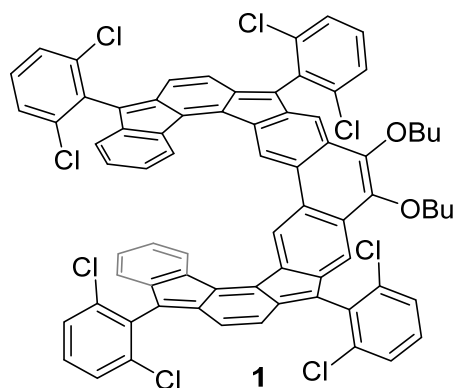
1

To an oven dried flask was added THF (150 mL) and 2.6-dichloro-1-bromobenzene (1.12 g, 5 mmol). The mixture was cooled to 0 °C and isopropylmagnesium chloride (2.0 M, 2 mL) was added slowly. The reaction was stirred for 2 h and then the compound **13** (100 mg, 0.1 mmol) was added quickly in one portion. The mixture was warmed to room temperature overnight. The reaction was quenched with saturated NH_4Cl solution and the organic phase was washed with water and then brine solution. The organic layer was dried over Na_2SO_4 and the volatiles removed. The crude product was then dissolved in 100 mL dry DCM under nitrogen atmosphere and 0.2 mL of $BF_3 \cdot OEt_2$ was added. The mixture was stirred for 30 minutes and quenched by methanol. The solvent was removed under reduced pressure. Under argon atmosphere and in the dark, the crude product was dissolved in 20 mL dry THF and tetrabutoxide potassium (10 equiv., 112 mg, 1 mmol) and 18-crown-6 (10 equiv., 264 mg 1 mmol) were added. The resulting mixture was stirred at room temperature for 24 h, then p-chloranil (5 equiv., 127 mg, 0.5 mmol) was added, and the mixture was stirred for an additional 30 min. Then the solvent was removed under reduced pressure at room temperature and the resulting

residue was directly subjected to flash chromatography (silica gel was neutralized with Et₃N, DCM/Hexane = 1:3). Black solid **1** was obtained in 84% yield (105 mg). ^{1}H NMR (500 MHz, THF-d_8): δ (ppm) 9.30 (s, 2H), 8.22 (d, J = 7.4 Hz, 2H), 7.63 (d, J = 7.8 Hz, 6H), 7.58 (d, J = 8.1 Hz, 4H), 7.51 (t, J = 8.1 Hz, 2H), 7.45 (t, J = 8.1 Hz, 2H), 7.04 (t, J = 7.4 Hz, 2H), 6.86 (d, J = 7.45 Hz, 2H), 6.68 (t, J = 7.4 Hz, 2H), 6.46-6.40 (m, 4H), 4.16 (t, J = 6.1 Hz, 4H), 1.72-1.68 (m, 4H), 1.50-1.42 (m, 4H), 0.91 (t, J = 7.4 Hz, 6H); HR-MS analysis (APCI): calcd for $C_{74}H_{46}Cl_8O_2$ (M+H)$^+$: 1247.1073; found, 1247.1069 (error: -0.5 ppm).
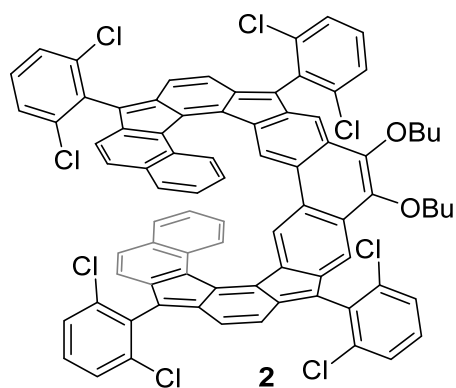
To an oven dried flask was added THF (150 mL) and 2.6-dichloro-1-bromobenzene (1.12 g, 5 mmol). The mixture was cooled to 0 °C and isopropylmagnesium chloride (2.0 M, 2 mL) was added slowly. The reaction was stirred for 2 h and then the compound **14** (100 mg, 0.091 mmol) was added quickly in one portion. The mixture was warmed to room temperature overnight. The reaction was quenched with saturated NH₄Cl solution and the organic phase was washed with water and then brine solution. The organic layer was dried over Na₂SO₄ and the volatiles removed. The crude product was then dissolved in 100 mL dry DCM under nitrogen atmosphere and 0.2 mL of BF₃·OEt₂ was added. The mixture was stirred for 30 minutes and quenched by methanol. The solvent was removed under reduced pressure. Under argon atmosphere and in the dark, the crude product was dissolved in 20 mL dry THF and tetrabutoxide potassium (10 equiv., 100 mg, 0.91 mmol) and 18-crown-6 (10 equiv., 240 mg, 0.91 mmol) were added. The resulting mixture was stirred at room temperature for 24 h, then p-chloranil (5 equiv., 116 mg, 0.46 mmol) was added, and the mixture was continued stirred for 30 min. Then the solvent was removed under reduced pressure at room temperature and the resulting residue was directly subjected to flash chromatography (silica gel was neutralized with Et₃N, DCM/Hexane = 1:3). Black solid **2** was obtained in 83% yield (102 mg). ^{1}H NMR (500 MHz, THF-d_8): δ (ppm) 7.79 (s, 2H), 7.68 (d, J = 8.0 Hz, 2H), 7.63 (t, J = 8.3 Hz, 4H), 7.58 (d, J = 8.1 Hz, 2H), 7.56 (d, J = 8.3 Hz, 2H), 7.50 (t, J = 8.7 Hz, 4H), 7.68 (d, J = 6.1 Hz, 2H), 7.46 (s, 2H), 7.09 (d, J = 8.1 Hz, 2H), 6.99 (d, J = 8.2 Hz, 2H), 6.76 (t, J = 7.1 Hz, 2H), 6.70 (td, ^3J = 8.2 Hz, ^4J = 1.5 Hz, 2H), 6.41 (d, J = 9.2 Hz, 2H), 6.30 (d, J = 9.2 Hz, 2H), 4.18-4.08 (m, 4H), 1.73-1.71 (m, 4H), 1.50-1.42 (m, 4H), 0.92 (t, J = 7.4 Hz, 6H); HR-MS analysis (APCI): calcd for $C_{82}H_{50}Cl_8O_2$ (M+H)$^+$: 1347.1369; found, 1347.1392 (error: 1.7 ppm).

1.3. Chemical titration of 1 and 2

Typical oxidation procedure to radical cation and dication: NO•SbF₆ (1 equiv. for radical cation, 2 equiv. for dication) dissolved in acetonitrile (50 μl) was added into the dry DCM solution of **1** or

2. The oxidized compounds were formed in 5 mins, and the solvent was removed under vacuum to give the radical cation and dication without further purification.

Typical reduction procedure to radical anion and dianion: The freshly prepared sodium anthracenide solution (0.1 M in dry THF, 1 equiv. for radical anion, 2 equiv. for dianion) was added dropwise to dry THF solution of **1** or **2**. The reduced compounds were in situ formed in 5 mins without further purification.
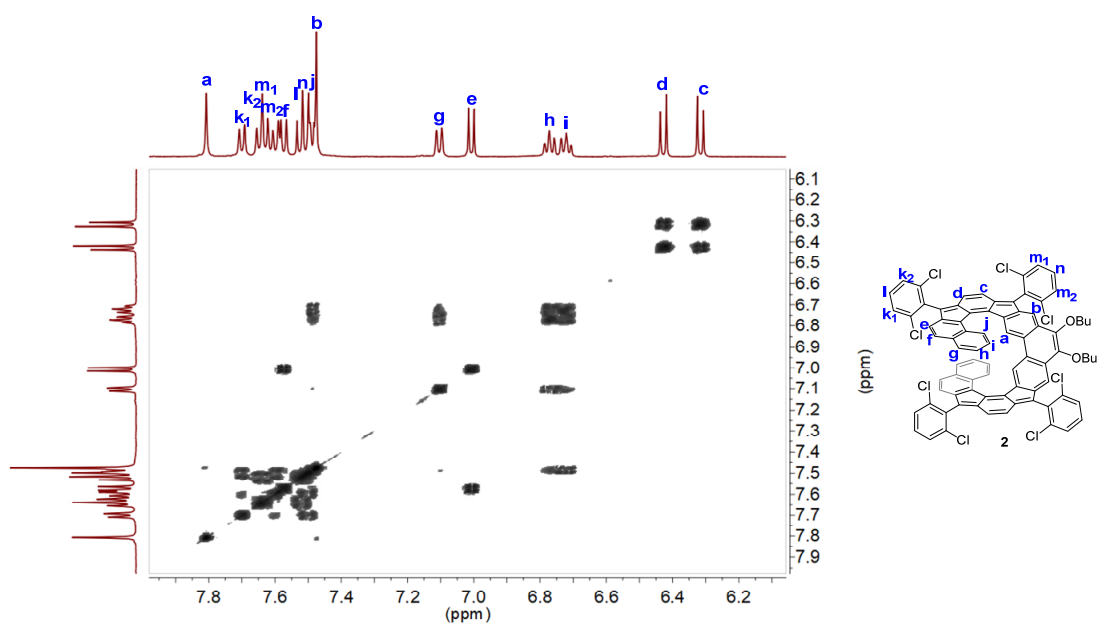
1.4 Additional spectrum
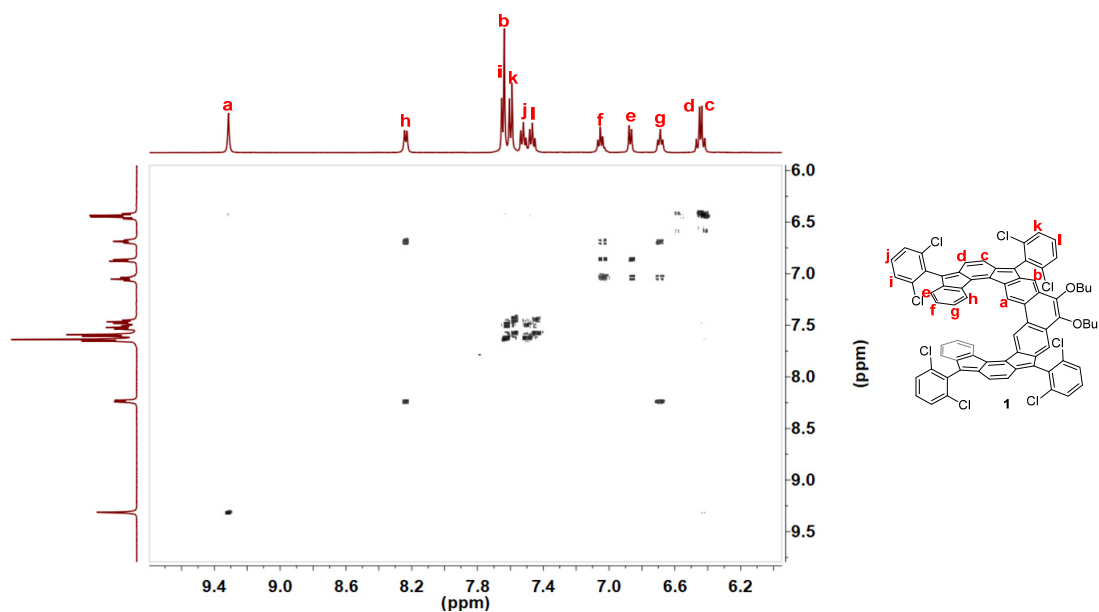
Figure S1. 2D COSY NMR (500 MHz) spectrum of compound **1** in THF-*d₈* at 298 K.
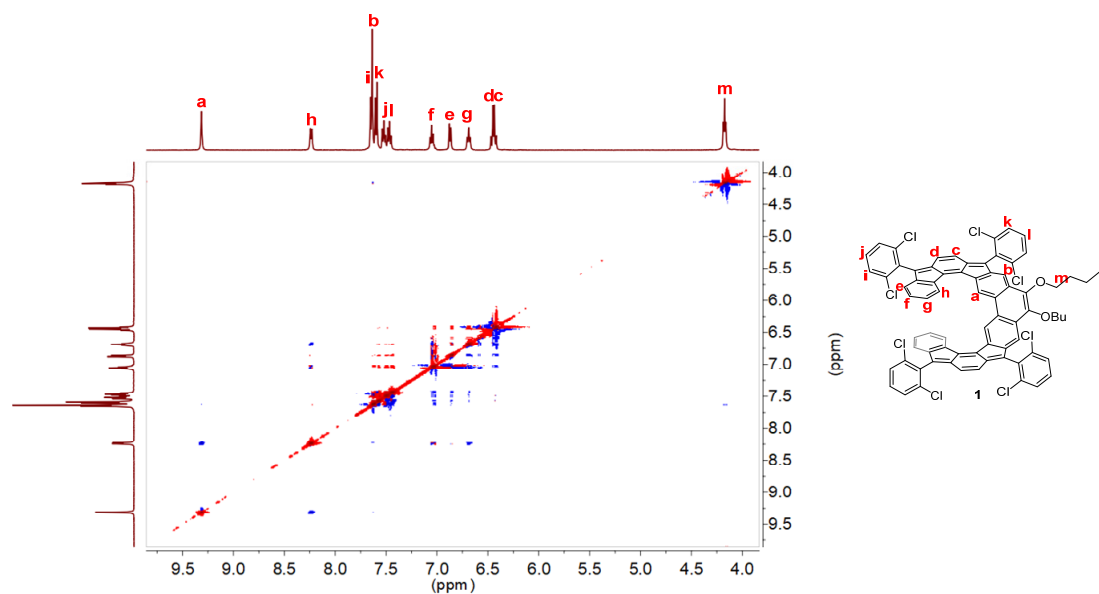
Figure S2. 2D ROESY NMR (500 MHz) spectrum of compound **1** in THF-*d₈* at 298 K.

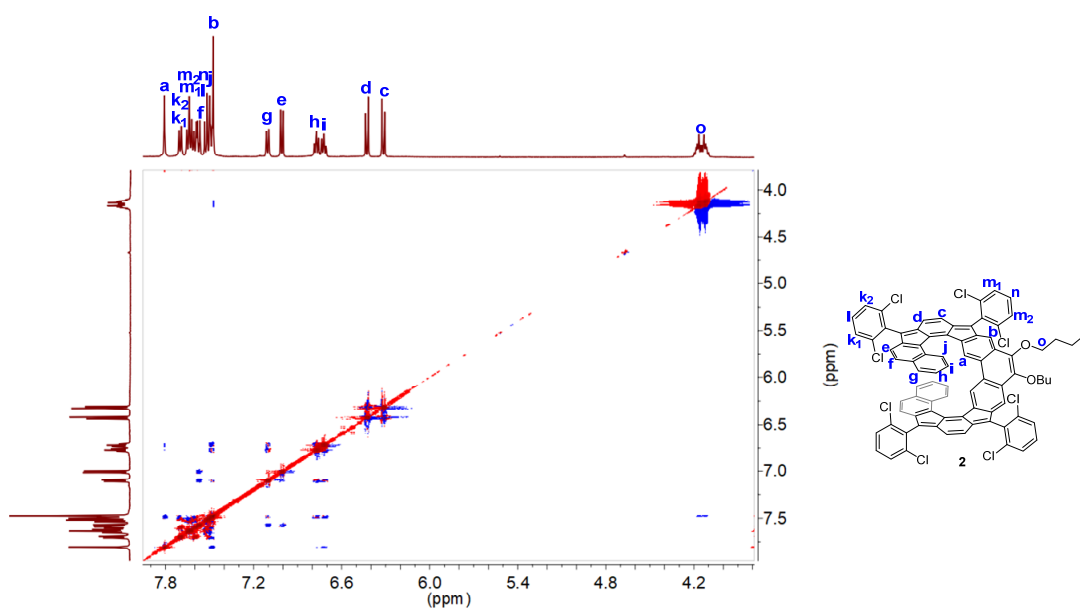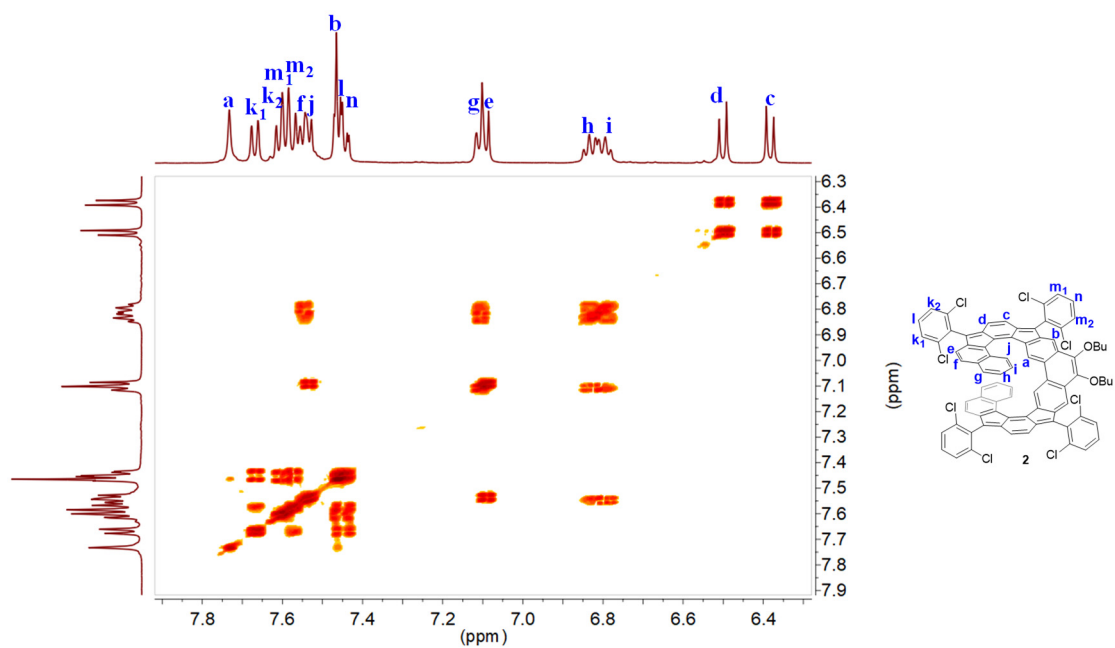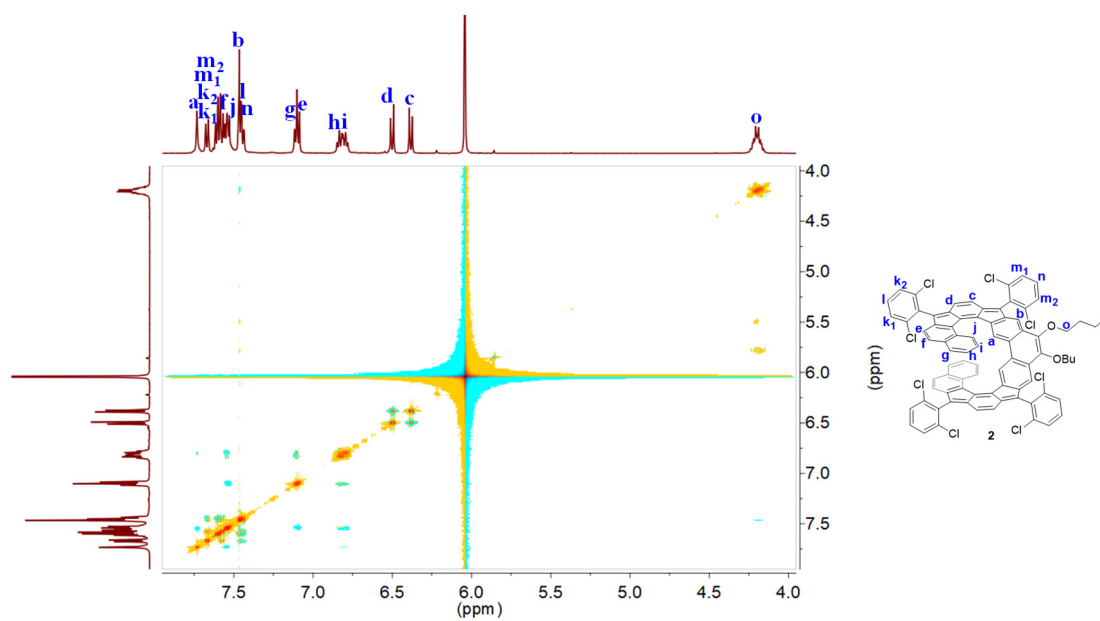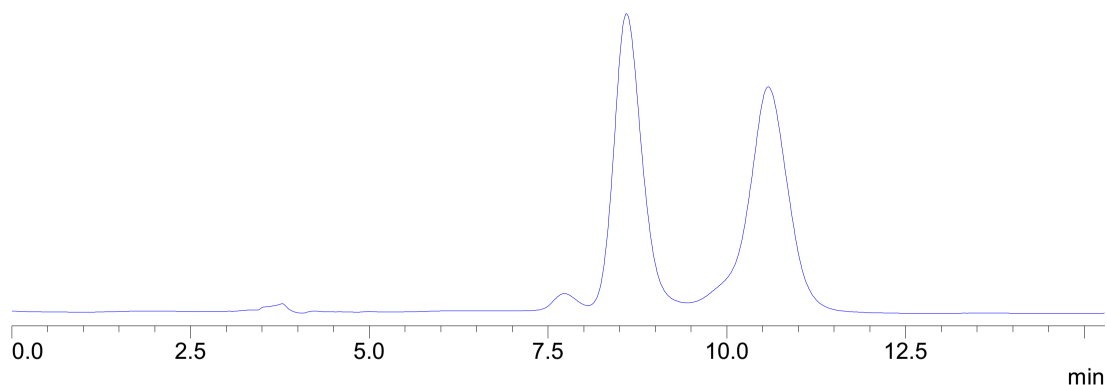**Figure S3.** 2D COSY NMR (500 MHz) spectrum of compound **2** in THF-*d₈* at 298 K.

**Figure S4.** 2D ROESY NMR (500 MHz) spectrum of compound **2** in THF-*d₈* at 298 K.

Figure S5. 2D COSY NMR (500 MHz) spectrum of compound **2** in C₂D₂Cl₄ at 300 K.

Figure S6. 2D ROESY NMR (500 MHz) spectrum of compound **2** in C₂D₂Cl₄ at 300 K.

Figure S7. Chiral HPLC chromatogram of **2**. (Column: CHIRALPAK ID (4.6 x 250 mm x 5μ); UV detector: 275 nm; Mobile phase: Hexane:IPA (65/35, v/v); Flow rate: 1.0 mL/min). *Note that **2** is soluble in DCM, chloroform, THF, EA and toluene, while it is slightly soluble in hexane, alcohols and acetonitrile. Therefore, the poor solubility of a mixture of **2** in mobile phase (Hexane/IPA) hampered large-scale preparative HPLC separation.*
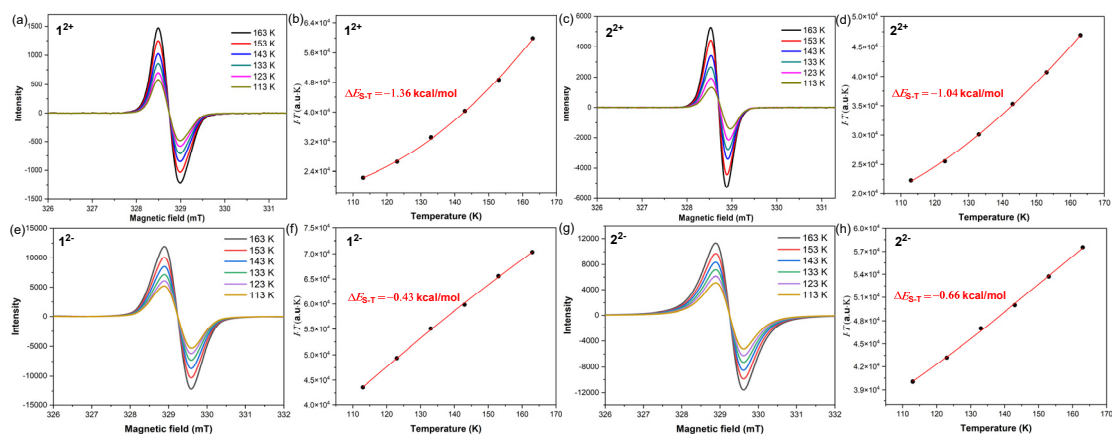
Figure S8. VT ESR spectra and fitted $I \times T - T$ curves by using Bleaney-Bowers equation of compounds 1^{2+} (a, b), 2^{2+} (c, d) 1^{2-} (e, f), and 2^{2-} (g, h) in frozen solution.

2. Estimation of the energy barrier for the isomerization process

The exchange rate constant k was estimated according to the literature.[1] Three characteristic exchange regions were observed in all cases if available: (1) a slow exchange region, in which the exchange is slower than the spectrometer timescale and two separate peaks are observed; (2) coalescence, at which two peaks completely merge into one peak; and (3) fast exchange region, in which the exchange is rapid than the spectrometer and the two peaks are merged into one peak. Therefore, the exchange rate constant k can be calculated by individual equation in these three regions.

(i) At slow exchange temperature ($T < T$c), two peaks are separated enough, the rate constant k can be determined by comparing the linewidth of a peak with no exchange with the line width of the peak with little exchange using the following formula: $k = \pi[(\Delta v_e)_{\frac{1}{2}} - (\Delta v_0)_{\frac{1}{2}}].$

(ii) For the coalescence temperature ($T = T_c$) k can be calculated using: $k = \frac{\pi}{\sqrt{2}}(\Delta v_0)$.

(iii) When temperature is close to T_c, two separated peaks will overlap with each other but not fully coalescent, thus the exchange constant at this temperature can then be calculated by: $k = \frac{\pi}{\sqrt{2}}[(\Delta v_0)^2 - (\Delta v_e)^2]^{1/2}$

At fast exchange temperature ($T > T_c$): $k = \frac{\pi(\Delta v_0)^2}{\sqrt{2}}\left[(\Delta v_e)_{\frac{1}{2}} - (\Delta v_0)_{\frac{1}{2}}\right]^{-1}$.

In these equations, Δv is the difference in chemical shift (Hz) between two correlated peaks at one temperature in the slow exchange region. Δv_0 is defined as the value of Δv at no exchange temperature (at which the two peaks are mostly separated), and Δv_e is defined as the value of Δv at all other temperatures in this region if available. $(\Delta v)_{1/2}$ is the linewidth (Hz) at half height of peak at anyone temperature in all region if available. $(\Delta v_0)_{1/2}$ is defined as the value of $(\Delta v)_{1/2}$ at no exchange temperature. $(\Delta v_e)_{1/2}$ is defined as the value of $(\Delta v)_{1/2}$ at all other temperatures in all region if available. T_c is defined as coalescence temperature at which two peaks completely merge into one peak. The obtained k values were then fitted with Eyring equation: $\ln\frac{k}{T} = \frac{-\Delta H^{\ddagger}}{R} \times \frac{1}{T} + \ln\frac{k_B}{h} + \frac{\Delta S^{\ddagger}}{R}$.

And then $\Delta G^{\ddagger} = \Delta H^{\ddagger} - T\Delta S^{\ddagger}$.

Table S1. Parameters obtained from the line-shape analysis based on the VT ^{1}H NMR spectra of **2** in THF-d_8.

T (K)	$(\Delta v_e)_{1/2}$ (Hz)	Δv_e (Hz)	k (s^{-1})
360	*Coalescence Temperature*		69.19802
350	-	27.62	28.26567
340	17.912	28.77	21.36287
330	13.766	29.04	8.33787
320	12.014	29.38	2.83372
310	11.424	29.67	0.98018
300	11.222	30.35	0.34558
290	11.112 (($\Delta v_0)_{1/2}$)	31.15 (Δv_0) **for the separated peak**	

3. DFT calculations

Theoretical calculations were performed with the Gaussian09 rev. D program suite.[2] All calculations were carried out using the density functional theory (DFT) method with Becke's three-parameter hybrid exchange functionals and the Lee-Yang-Parr correlation functional (B3LYP) employing the 6-31G(d,p) basis set for all atoms.[3] Natural orbital occupation number (NOON)) calculations were done by spin unrestricted LC-BLYP/6-31G(d) method and the diradical character (y_0) was calculated according to Yamaguchi's scheme: $y_0 = 1 - (2T/(1 + T^2))$, and $T = (n_{HONO} - n_{LUNO})/2$ (n_{HOMO} is the occupation number of the HONO, n_{LUNO} is the occupation number of the LUNO).[4] Time-dependent DFT (TD-DFT) calculations have been performed at the (R)B3LYP/6-31G(d,p) or (U)B3LYP/6-31G(d,p) level of theory. NICS values were calculated using the standard GIAO procedure.[5] AICD plot was calculated by using the method developed by Herges.[6]

Electrostatic potential maps and Mulliken charge were calculated at the B3LYP/6-31G(d,p).

In the study of isomerization and racemization processes, molecular geometries of all stationary points were optimized at the B3LYP level of DFT with the 6-31G(d) basis set with IEPCM model as solvation of THF. Harmonic vibration frequency calculations at the same level were performed to verify all stationary points as local minima (with no imaginary frequency) or transition states (with one imaginary frequency). IRC calculations[7] were also performed to check transition states.

Table S2. Summary of energy of local minimum states and transition states during isomerization process of **1** (Hartree).[a]

	E (H.F)	$E + ZPE$ (H.F)	H (H.F)	G (H.F)
(M,M)-1	-6443.746008	-6442.938882	-6442.873759	-6443.051332
(P,M)-1	-6443.743153	-6442.936073	-6442.871034	-6443.046159
TS-1A	-6443.742205	-6442.936080	-6442.872345	-6443.044066
TS-1B	-6443.734994	-6442.928403	-6442.864162	-6443.036740

(a) E: electronic energy; ZPE: zero-point energy; H ($= E + ZPE + E_{vib} + E_{rot} + E_{trans} + RT$): sum of electronic and thermal enthalpies; G ($= H - TS$): sum of electronic and thermal free energies.

Table S3. Summary of energy of local minimum states and transition states during isomerization process of **2** (Hartree).[a]

	E (H.F)	$E + ZPE$ (H.F)	H (H.F)	G (H.F)
(M,M)-2	-6751.014390	-6750.114266	-6750.043822	-6750.229372
(P,M)-2	-6751.002451	-6750.102273	-6750.031855	-6750.218471
TS-2A	-6750.990149	-6750.090624	-6750.020614	-6750.206293
TS-2B	-6750.985647	-6750.086568	-6750.016882	-6750.199501

(b) E: electronic energy; ZPE: zero-point energy; H ($= E + ZPE + E_{vib} + E_{rot} + E_{trans} + RT$): sum of electronic and thermal enthalpies; G ($= H - TS$): sum of electronic and thermal free energies.
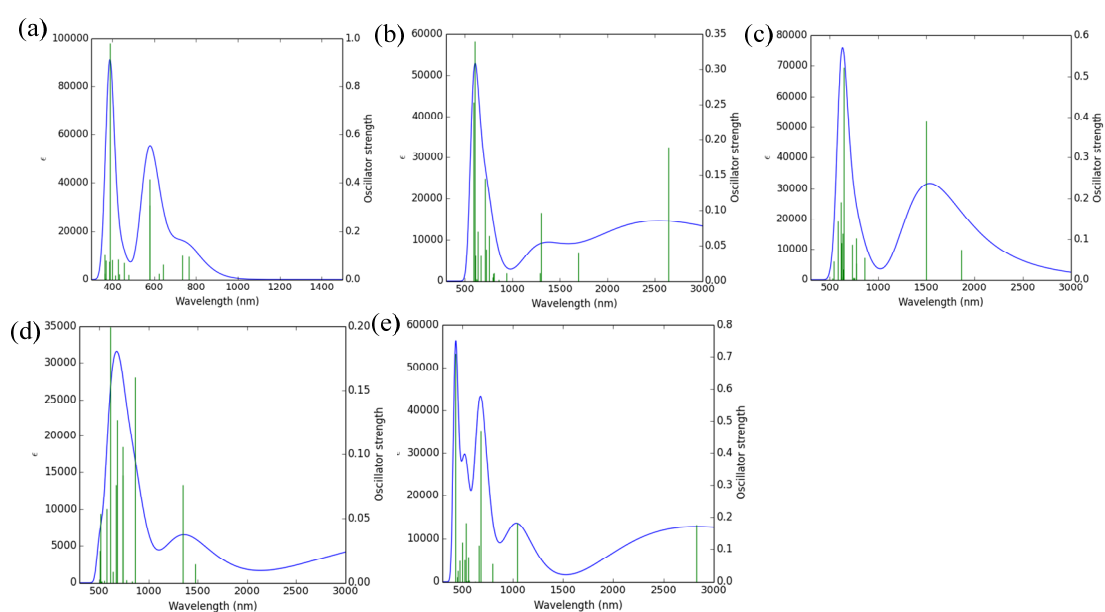
Figure S9. TD DFT simulated spectra of **1** (a), **1**[.+] (b), **1**[2+] (c) **1**[.-] (d), and **1**[2-] (e).

Table S4. Selected TD-DFT (RB3LYP/6-31G(d,p)) calculated energies, oscillator strength and compositions of major electronic transitions of **1**. H=HOMO, L=LUMO, L+1=LUMO+1, etc.

Wavelength (nm)	Osc. Strength (*f*)	Major contributions
764.2	0.0962	H->L (90%), H-2->L+1 (7%)
735.1	0.1007	HOMO->L+1 (91%), H-2->L (7%)
577.2	0.4137	H-2->L (61%), H-1->L (31%)
577.1	0.3059	H-2->L+1 (89%), H->L (7%)
456.6	0.0704	H-4->L+1 (12%), H-3->L+1 (73%), H-5->L (8%)
429.1	0.0857	H-4->L+1 (69%), H-3->L+1 (12%), H->L+2 (10%)
389.8	0.9817	H->L+2 (73%), H-6->L (6%), H-5->L (4%), H-4->L+1 (6%)

Table S5. Selected TD-DFT (UB3LYP/6-31G(d,p)) calculated energies, oscillator strength and compositions of major electronic transitions of **1·+**. H=HOMO, L=LUMO, L+1=LUMO+1, etc.

Wavelength (nm)	Osc. Strength (*f*)	Major contributions
2644.1	0.1895	H (B)->L (B) (95%), H(A)->L(A) (2%), H-1(B)->L(B) (3%)
1299.8	0.0963	H-1(A)->L+1(A) (18%), H(A)->L(A) (53%), H(B)->L+2(B) (24%)
754.1	0.0641	H-2(A)->L(A) (12%), H(A)->L+1(A) (45%), H-1(B)->L+1(B) (12%), H-3(A)->L+1(A) (2%), H-1(A)->L(A) (8%)
712.7	0.1453	H-1(A)->L(A) (48%), H-1(B)->L+1(B) (17%), H(B)->L+1(B) (23%)
602.5	0.3403	H-3(A)->L+1(A) (10%), H-2(A)->L(A) (24%), H-1(B)->L+1(B) (31%) H-5(A)->L(A) (5%), H-1(A)->L(A) (8%)
592.3	0.2526	H-2(A)->L+1(A) (40%), H-1(B)->L+2(B) (46%)

Table S6. Selected TD-DFT (RB3LYP/6-31G(d,p)) calculated energies, oscillator strength and compositions of major electronic transitions of **1²⁺**. H=HOMO, L=LUMO, L+1=LUMO+1, etc.
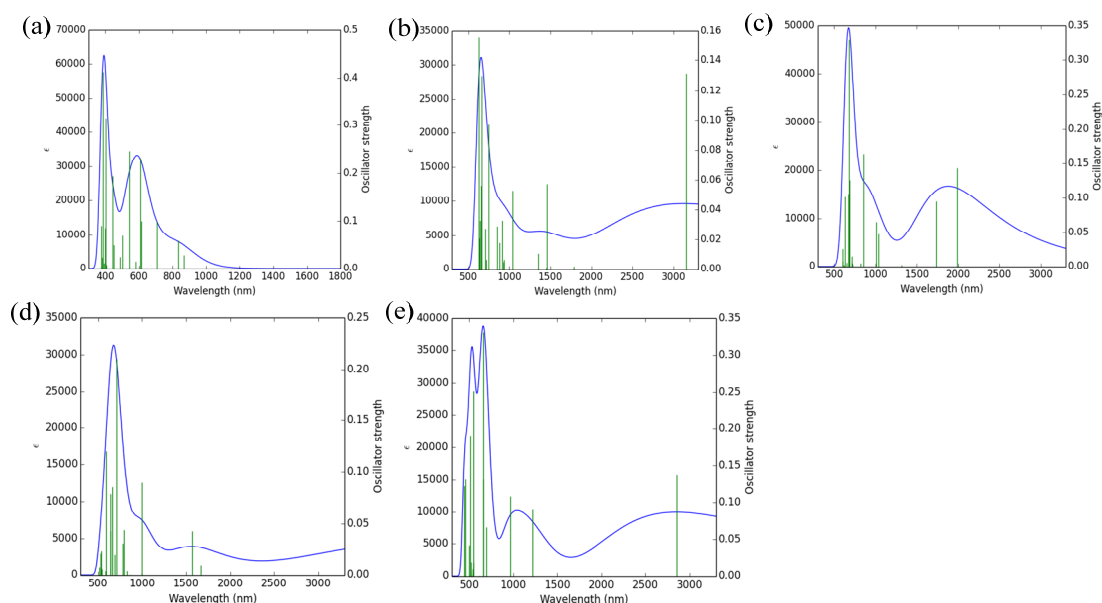
Wavelength (nm)	Osc. Strength (*f*)	Major contributions
1860.2	0.074	H-1->L (64%), H->L (38%)
1502.2	0.3899	H-1->L (35%), H->L (69%)
775.2	0.102	H-3->L (53%), H-1->L+1 (26%), H->L+1 (13%)
730.0	0.0861	H-8->L (11%), H->L+2 (75%) H-13->L (3%)
645.1	0.521	H-11->L (21%), H-1->L+1 (46%), H->L+1 (14%)
632.7	0.1142	H-10->L (79%), H-1->L+2 (17%)
615.2	0.191	H-10->L (16%), H-1->L+2 (74%)

Table S7. Selected TD-DFT (UB3LYP/6-31G(d,p)) calculated energies, oscillator strength and compositions of major electronic transitions of **1·⁻**. H=HOMO, L=LUMO, L+1=LUMO+1, etc.

Wavelength (nm)	Osc. Strength (*f*)	Major contributions
4953.4	0.0953	H (A)->L (A) (102%)
1476.8	0.0143	H-1(A)->L (A) (56%), H-1(B)->L (B) (14%), H (B)->L+1(B)
867.4	0.16	H-1(A)->L (A) (37%), H (B)->L+1(B) (56%), H-2(B)->L (B)
739.3	0.106	H (A)->L+1(A) (80%) H-3(A)->L (A) (7%), H-2(A)->L (A) (2%), H-2(B)->L+1(B) (5%), H-1(B)->L+1(B) (2%)
612.6	0.1993	H-3(A)->L (A) (26%), H-2(B)->L+1(B) (57%), H-6(A)->L (A) (2%), H-3(B)->L (B) (7%), H (B)->L (B) (2%)
509.8	0.0536	H (A)->L+5(A) (88%) H-5(A)->L (A) (3%), H (A)->L+8(A) (2%)

Table S8. Selected TD-DFT (RB3LYP/6-31G(d,p)) calculated energies, oscillator strength and compositions of major electronic transitions of **1²⁻**. H=HOMO, L=LUMO, L+1=LUMO+1, etc.

Wavelength (nm)	Osc. Strength (*f*)	Major contributions
2827.4	0.177	H->L (130%)
1045.0	0.1834	H-1->L (98%)
683.7	0.4718	H->L+1 (92%) H-2->L (6%), H->L (2%)
663.3	0.1112	H-3->L (96%), H-2->L (2%)
534.3	0.1834	H->L+7 (86%), H-4->L (2%), H->L+6 (8%)
432.1	0.7097	H-1->L+1 (46%), H->L+12 (43%), H-5->L (3%)

Figure S10. TD DFT simulated spectra of **2** (a), **2**$^{·+}$ (b), **2**$^{2+}$ (c) **2**$^{·-}$ (d), and **2**$^{2-}$ (e).

Table S9. Selected TD-DFT (RB3LYP/6-31G(d,p)) calculated energies, oscillator strength and compositions of major electronic transitions of **2**. H=HOMO, L=LUMO, L+1=LUMO+1, etc.

Wavelength (nm)	Osc. Strength (*f*)	Major contributions
867.5	0.0277	H-1->L+1 (13%), H->L (83%)
834.5	0.0597	H-1->L (21%), H->L+1 (72%)
609.7	0.2323	H-2->L (84%), H-4->L (2%), H-3->L+1 (6%)
544.6	0.2469	H-3->L+1 (87%), H-2->L (3%), H-1->L (3%)
445.0	0.1939	H-5->L (72%), H-4->L+1 (16%) H-7->L+1 (4%)
402.9	0.315	H-7->L (19%), H->L+2 (65%) H-6->L+1 (9%)
385.4	0.412	H-7->L (35%), H-6->L+1 (25%), H->L+2 (24%)

Table S10. Selected TD-DFT (UB3LYP/6-31G(d,p)) calculated energies, oscillator strength and compositions of major electronic transitions of **2**$^{·+}$. H=HOMO, L=LUMO, L+1=LUMO+1, etc.

Wavelength (nm)	Osc. Strength (*f*)	Major contributions
3157.2	0.1314	H(B)->L(B) (97%)
1456.7	0.057	H-1(A)->L+1(A) (19%), H(A)->L(A) (50%), H(B)->L+2(B) (25%)
1038.4	0.0525	H-3(B)->L(B) (86%) H-1(A)->L+1(A) (2%), H(A)->L(A) (4%), H-2(B)->L+1(B) (2%), H-1(B)->L+2(B) (3%)
749.1	0.0971	H-1(A)->L+1(A) (62%), H(A)->L(A) (11%)
661.1	0.1298	H-9(B)->L(B) (24%), H-5(B)->L(B) (46%) H-3(A)->L(A) (4%), H-2(A)->L+1(A) (4%), H-7(B)->L(B) (3%), H-2(B)->L+1(B) (9%), H-1(B)->L+2(B) (4%)
629.2	0.1559	H-2(A)->L(A) (16%), H-2(B)->L+2(B) (14%), H-1(B)->L+1(B) (44%), H-3(A)->L+1(A)

(2%), H-10(B)->L(B) (9%), H-8(B)->L(B) (2%), H-3(B)->L+1(B) (6%)

Table S11. Selected TD-DFT (RB3LYP/6-31G(d,p)) calculated energies, oscillator strength and compositions of major electronic transitions of **2^{2+}**. H=HOMO, L=LUMO, L+1=LUMO+1, etc.

Wavelength (nm)	Osc. Strength (*f*)	Major contributions
1989.7	0.1437	H-1->L (28%), H->L (78%)
857.2	0.1643	H->L+2 (84%), H-3->L (8%), H->L (2%)
684.1	0.1261	H-2->L+1 (83%) H-1->L+2 (9%), H->L (2%)
679.3	0.3302	H-4->L (11%), H-2->L+2 (10%), H-1->L+1 (55%)
672.6	0.1057	H-2->L+1 (11%), H-1->L+2 (85%)
633.8	0.1019	H-9->L (90%), H-12->L (2%)
601.7	0.0251	H-13->L (54%), H-12->L (44%)

Table S12. Selected TD-DFT (UB3LYP/6-31G(d,p)) calculated energies, oscillator strength and compositions of major electronic transitions of **2$^{\cdot-}$**. H=HOMO, L=LUMO, L+1=LUMO+1, etc.

Wavelength (nm)	Osc. Strength (*f*)	Major contributions
5530.0	0.073	H (A)->L (A) (101%)
1666.2	0.0093	H-1(A)->L (A) (56%), H-1(B)->L (B) (16%), H (B)->L+1(B) (29%)
999.6	0.0892	H-1(A)->L (A) (42%), H-1(B)->L (B) (12%), H (B)->L+1(B) (41%), H-3(B)->L+1(B) (2%), H-2(B)->L (B) (3%)
782.7	0.031	2.907-A H-4(A)->L (A) (43%), H-2(B)->L (B) (18%), H-1(B)->L (B) (17%) H-1(A)->L (A) (2%), H-3(B)->L+1(B) (8%), H (B)->L+1(B) (6%)
709.2	0.2098	H (A)->L+1(A) (88%) H-1(B)->L+1(B) (4%)
589.3	0.1197	H-4(A)->L (A) (22%), H-4(B)->L (B) (13%), H-3(B)->L+1(B) (53%), H-6(A)->L (A) (2%), H-2(A)->L+2(A) (2%), H-1(A)->L+1(A) (2%)

Table S13. Selected TD-DFT (RB3LYP/6-31G(d,p)) calculated energies, oscillator strength and compositions of major electronic transitions of **2^{2-}**. H=HOMO, L=LUMO, L+1=LUMO+1, etc.

Wavelength (nm)	Osc. Strength (*f*)	Major contributions
2853.4	0.1374	H->L (120%), H-2->L (2%)
1216.8	0.0911	H-1->L (98%)
965.1	0.108	H-2->L (94%), H->L (3%)
659.3	0.331	H->L+1 (94%), H-5->L (2%)
657.0	0.132	H-4->L (95%)
548.6	0.2517	H-5->L (83%) H-3->L (3%), H->L+7 (5%)

| 514.5 | 0.1901 | H-6->L (34%), H->L+8 (13%), H->L+10 (48%) |
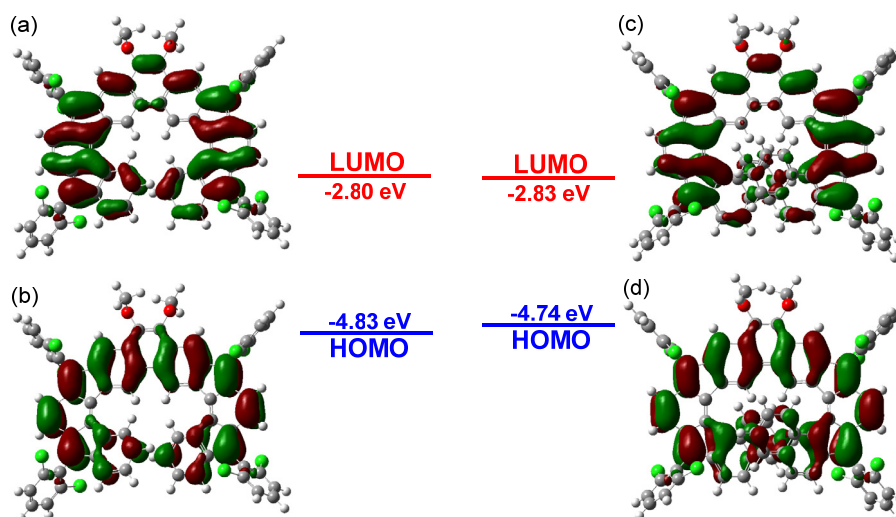
Figure S11. Energy diagrams of **1** and **2** (eV); and molecular orbitals (RB3LYP/6-31G(d,p)) of a) LUMO and b) HOMO of **1**, and c) LUMO and d) HOMO of **2**.
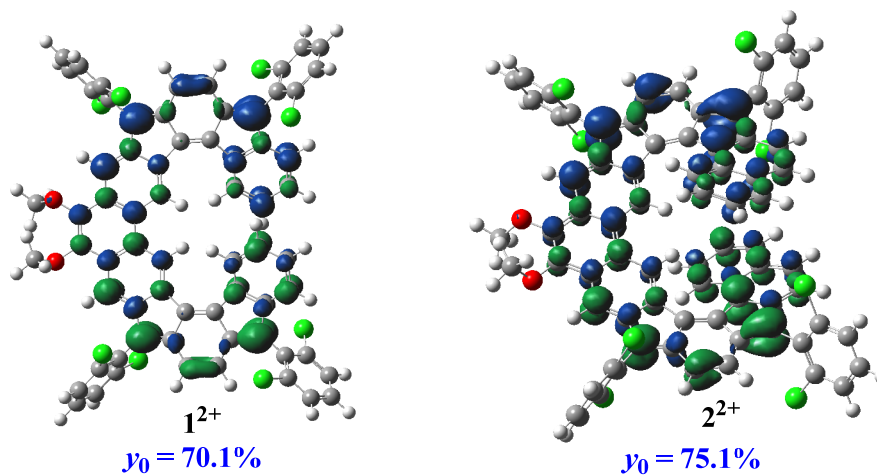

Figure S12. Calculated spin-density distribution (UCAM-B3LYP/6-31G(d)) of the singlet ground states of 1^{2+} and 2^{2+}, and their calculated diradical character (y_0). Blue and green surfaces represent α and β spin density, respectively.
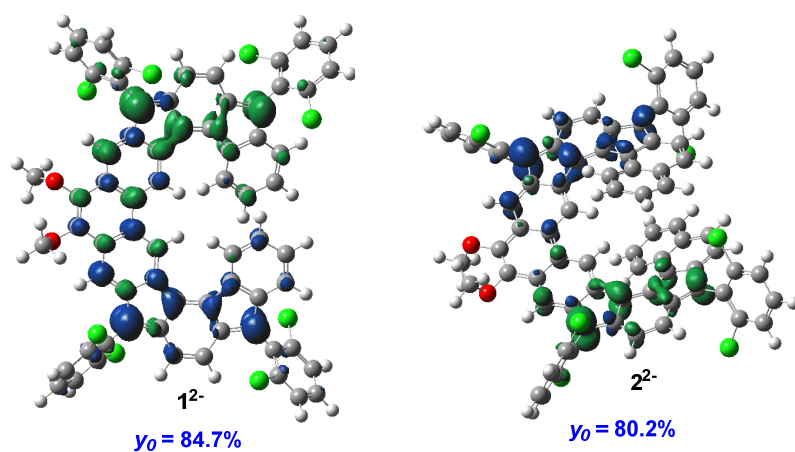
Figure S13. Calculated spin-density distribution (UCAM-B3LYP/6-31G(d)) of the singlet ground states of 1^{2-} and 2^{2-}, and their calculated diradical character (y_0). Blue and green surfaces represent α and β spin density, respectively.
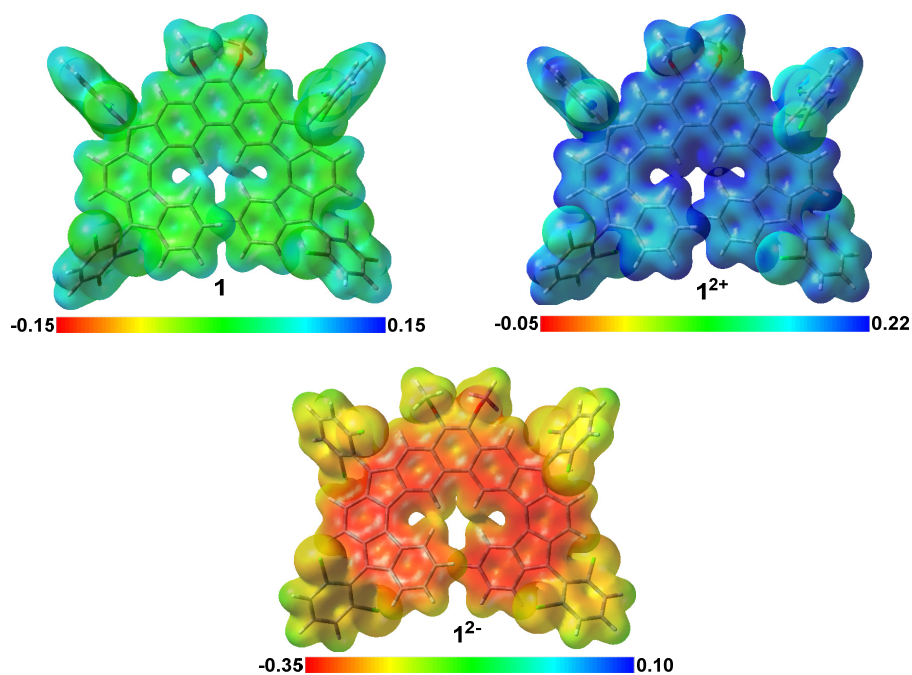
Figure S14. Calculated electrostatic potential maps for the compound **1** and its charged species. Red regions represent more negative charges, and blue regions represent more positive charges.
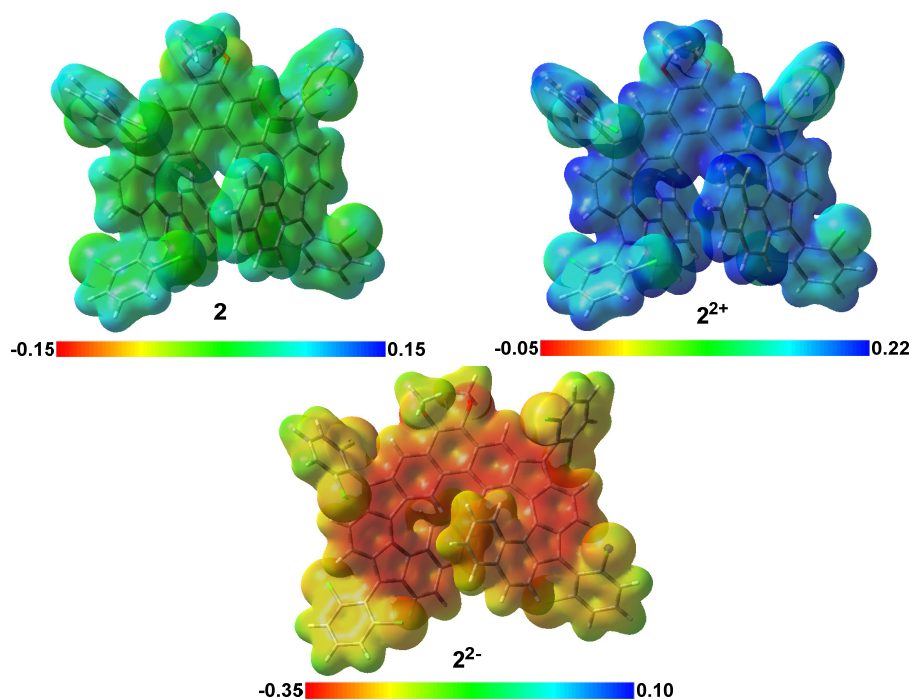
Figure S15. Calculated electrostatic potential maps for the compound **2** and its charged species. Red regions represent more negative charges, and blue regions represent more positive charges.
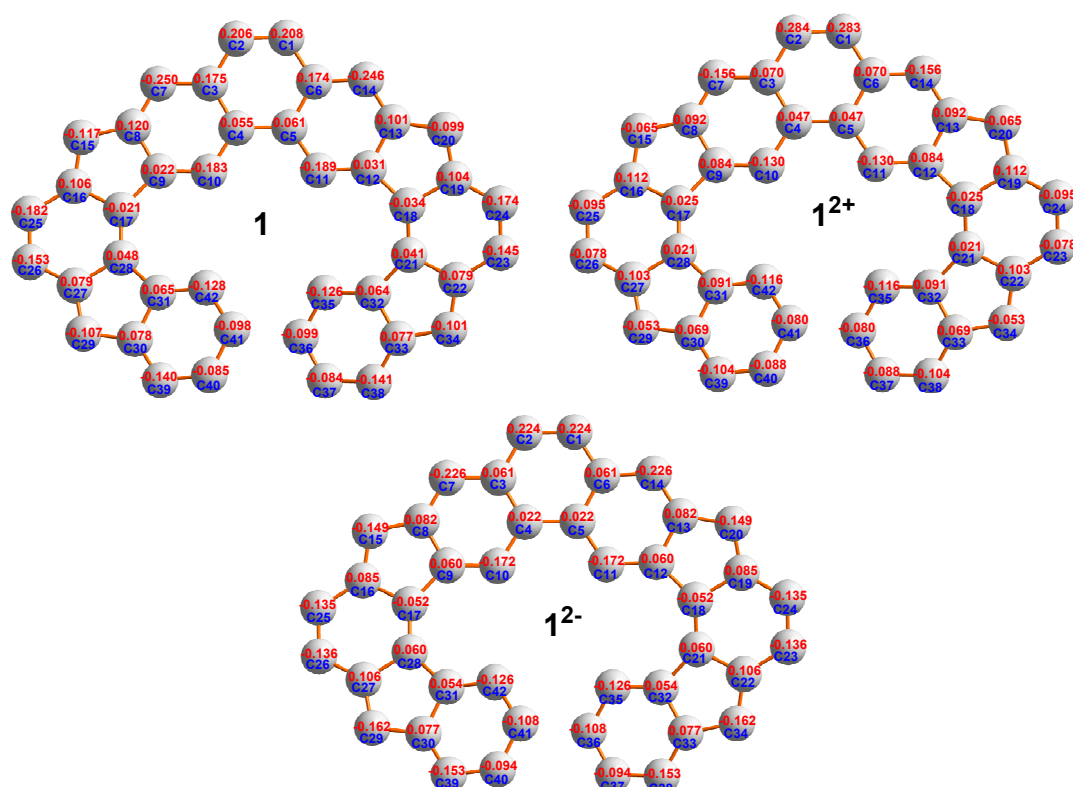
Figure S16. Mulliken charge distribution of **1** and its charged species.
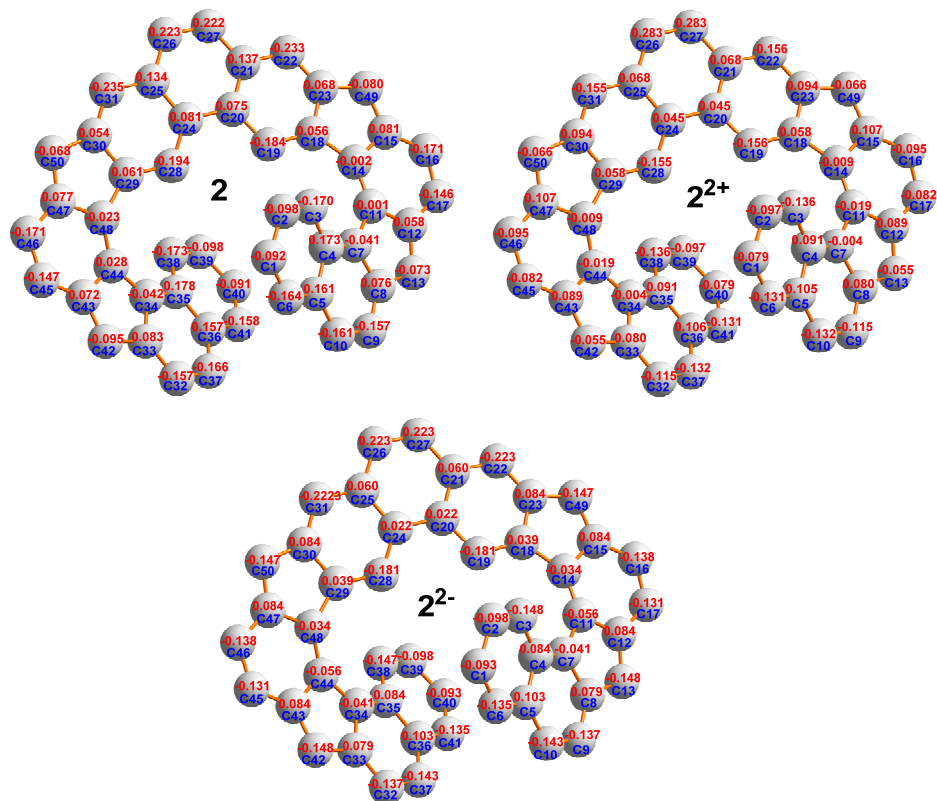
Figure S17. Mulliken charge distribution of **2** and its charged species.
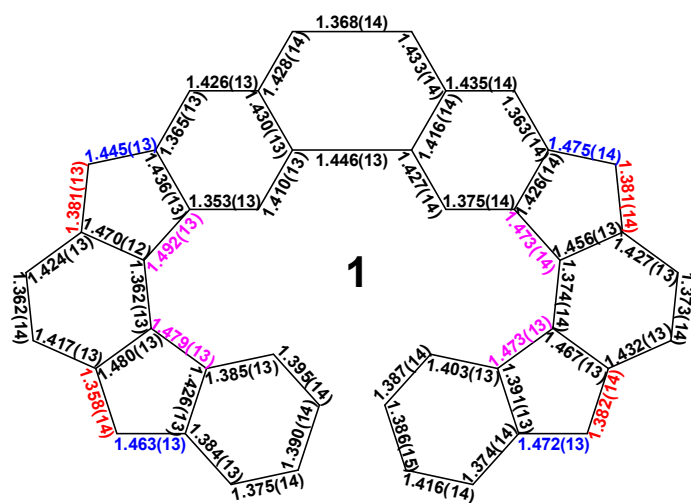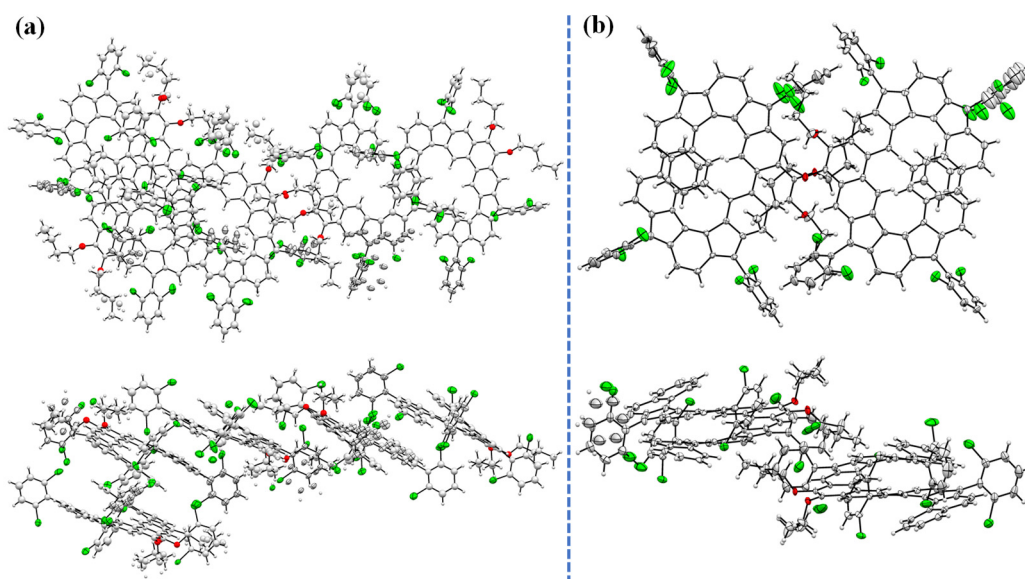
4. Crystallographic data of 1 and 2
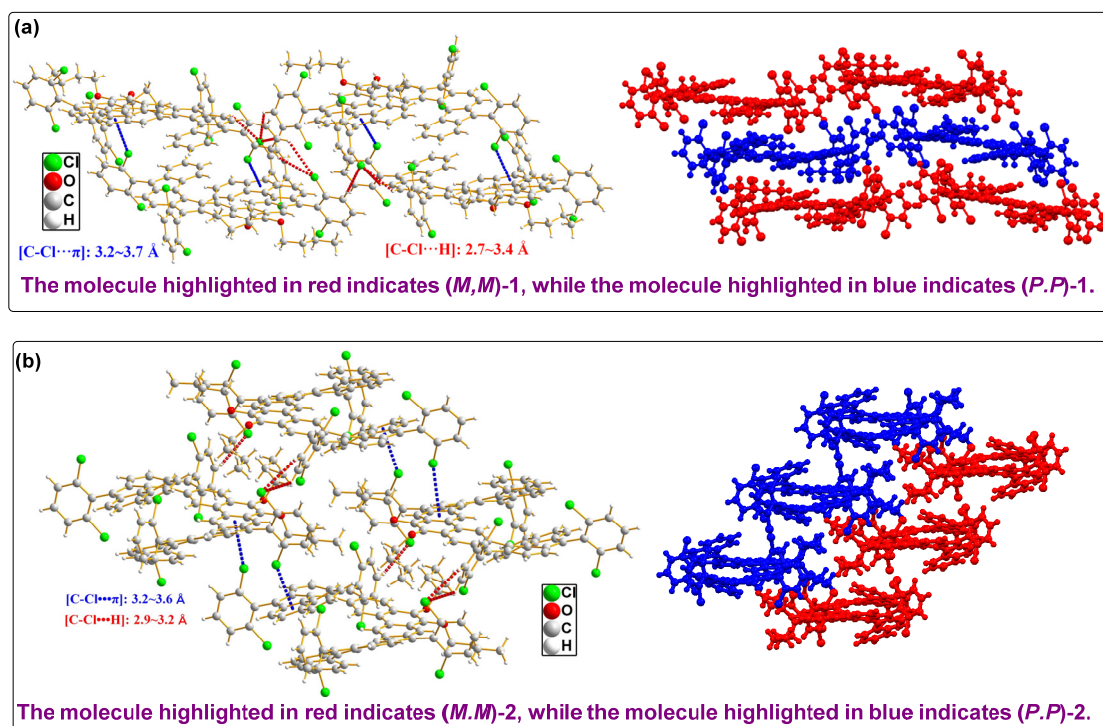
Figure S18. Molecular packing structures of **1** (a) and **2** (b).
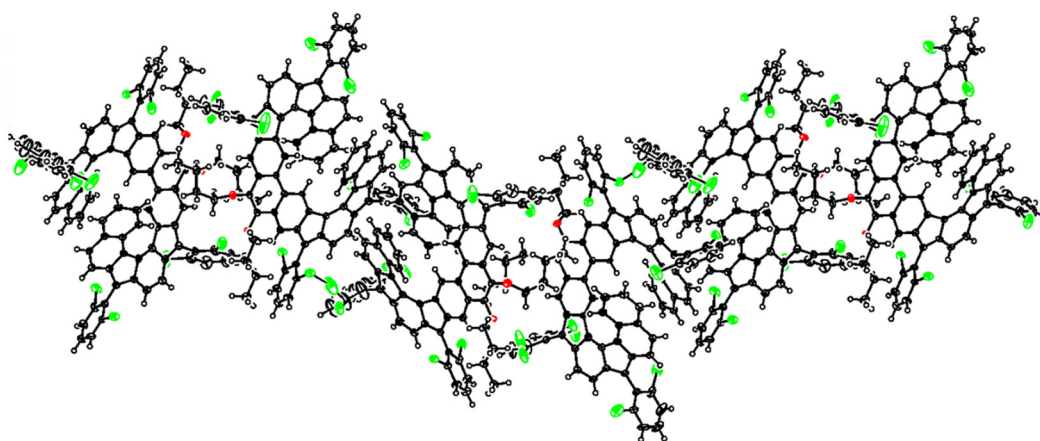
Figure S19. The structural drawing of **2** showing ADPs.

Figure S20. Selected bond lengths (Å) of compound **1** from the crystallographic data.

Figure S21. ORTEP drawing of (a) **1** and (b) **2**. The thermal ellipsoids are scaled to 50% probabilities.

Table S14. Crystal data and structure refinement for **1.**

Identification code	j027b_a_sq
Empirical formula	$C_{666}H_{414}Cl_{72}O_{18}$
Formula weight	11256.35
Temperature/K	100(2)
Crystal system	monoclinic
Space group	C2/c
a/Å	80.084(7)
b/Å	16.1201(13)
c/Å	54.564(4)
$\alpha/°$	90
$\beta/°$	129.561(4)
$\gamma/°$	90
Volume/Å^3	54306(8)
Z	4
$\rho_{calc}g/cm^3$	1.377
μ/mm^{-1}	3.793
F(000)	23112.0
Crystal size/mm^3	0.030 x 0.050 x 0.060 mm
Radiation	CuKα ($\lambda = 1.54178$)
2Θ range for data collection/°	4.2 to 133.19
Index ranges	$-95 \leq h \leq 90, -19 \leq k \leq 19, -61 \leq l \leq 64$
Reflections collected	423546
Independent reflections	47876 [$R_{int} = 0.1198$, $R_{sigma} = 0.0565$]
Data/restraints/parameters	47876/2128/2575
Goodness-of-fit on F^2	1.121
Final R indexes [I>=2σ (I)]	R1 = 0.1989, wR2 = 0.4306
Largest diff. peak/hole / e Å-3	2.92/-1.10

The low quality of the crystallographic data of compound 1 does not allow reliable bond length analysis, but the backbone of π-molecule was clearly seen.

The asymmetric unit contains 4.5 molecules of the compound $C_{74}H_{46}Cl_{18}O_2$ and many weak solvent peaks. In the first molecule, two butyl groups and a $Cl_2C_6H_3$ group were disordered into two positions with occupancy ratio = 66:34, 69:31 and 77:23 respectively. In the second molecule, two butyl groups, one dichlorophenyl ($Cl_2C_6H_3$) group and one $Cl_2C_{12}H_6$ group (including one dichlorophenyl group together with its adjacent C_6H_3 unit in the molecular backbone) were disordered into two positions with occupancy ratio = 75:25, 66:34, 76:24 and 79:21 respectively. In the third molecule, two $Cl_2C_6H_3$ groups and one $Cl_2C_{12}H_6$ group (including one dichlorophenyl group together with its adjacent C_6H_3 unit in the molecular backbone) were disordered into two positions with occupancy ratio = 54:46, 58:42 and 77:23 respectively. In the fourth molecule, one butyl group and two $Cl_2C_6H_3$ groups were disordered into two positions with occupancy ratio = 71:29, 77:23 and 51:49 respectively. In the fifth residue (0.5 molecule), one $Cl_2C_6H_3$ group was disordered into two positions with occupancy ratio = 60:40. All disordered atoms were modelled from the residual peaks. Restraints in bond lengths and thermal parameters were applied to the

disordered atoms. Most C and O atoms were refined isotropically. The diffused and weak solvent peaks in the lattice could not be modelled satisfactorily. Hence the regions were squeezed using Platon program. The total electron count in the voids was 204.

Alert level A PROBLEM: *Isotropic non-H Atoms in Main Residue(s) .... 300 Report*

RESPONSE: *As there are four and a half molecules in the asymmetric unit and many of them are disordered, hence some of the O and C are kept isotropic to keep the refinement data-to-parameter-ratio higher.*

Alert level B PROBLEM: *High R1 Value .... 0.20 Report*

RESPONSE: *The high R1 Value could be due to the crystal is a large macromolecule helical compound. The helical conformation and rigidity of the fused polyaromatic rings caused the crystal difficult to packed well. The unit cell was very large with four and half molecules in the asymmetric units. The crystal was not packed well so the data quality was poor. The reflection intensities were low. I/sigma = 3.3. As the crystal was not packed well, many segments of the molecules were disordered into two positions or even more.*

Alert level B PROBLEM: *High wR2 Value (i.e. > 0.25) .... 0.45 Report*

RESPONSE: *The high wR2 Value could be due the crystal is a large macromolecule helical compound. The helical conformation and rigidity of the fused polyaromatic rings caused the crystal difficult to packed well. The unit cell was very large with four and half molecules in the asymmetric units. The crystal was not packed well so the data quality was poor. The reflection intensities were low. I/sigma = 3.3. As the crystal was not packed well, many segments of the molecules were disordered into two positions or even more.*

Alert level B PROBLEM: *Large Reported Max. (Positive) Residual Density 2.92 eA-3*

RESPONSE: *This could be due to there were further disorder issues.*

Alert level B PROBLEM: *Low Bond Precision on C-C Bonds .... 0.01757 Ang.*

RESPONSE: *The Low Bond Precision on C-C Bonds could be due the crystal is a large macromolecule helical compound. The helical conformation and rigidity of the fused polyaromatic rings caused the crystal difficult to packed well. The unit cell was very large with four and half molecules in the asymmetric units. The crystal was not packed well so the data quality was poor. The reflection intensities were low. I/sigma = 3.3. As the crystal was not packed well, many segments of the molecules were disordered into two positions or even more.*

Alert level B PROBLEM: *Check Calcd Resid. Dens. 1.50Ang From Cl6A_3 2.86 eA-3*

RESPONSE: *This could be due to there were further disorder issues.*

Table S15. Crystal data and structure refinement for **2.**

Identification code	JQ004_0m_a
Empirical formula	$C_{82}H_{50}Cl_8O_2$
Formula weight	1350.82
Temperature/K	99.98
Crystal system	monoclinic
Space group	$P2_1/n$
a/Å	12.8626(6)
b/Å	40.918(2)
c/Å	29.4548(15)
α/°	90

β/°	101.243(3)
γ/°	90
Volume/Å^3	15205.0(13)
Z	8
ρ_{calc}g/cm^3	1.180
μ/mm^{-1}	3.048
F(000)	5552.0
Crystal size/mm^3	0.843 × 0.608 × 0.309
Radiation	CuKα (λ = 1.54184)
2Θ range for data collection/°	7.168 to 160.208
Index ranges	-14 ≤ h ≤ 16, -52 ≤ k ≤ 51, -37 ≤ l ≤ 37
Reflections collected	502851
Independent reflections	32390 [R_{int} = 0.1111, R_{sigma} = 0.0389]
Data/restraints/parameters	32390/33/1686
Goodness-of-fit on F^2	1.036
Final R indexes [I>=2σ (I)]	R_1 = 0.1036, wR_2 = 0.2427
Final R indexes [all data]	R_1 = 0.1126, wR_2 = 0.2494
Largest diff. peak/hole / e Å^{-3}	1.28/-1.18

5. NMR and HR MS spectra
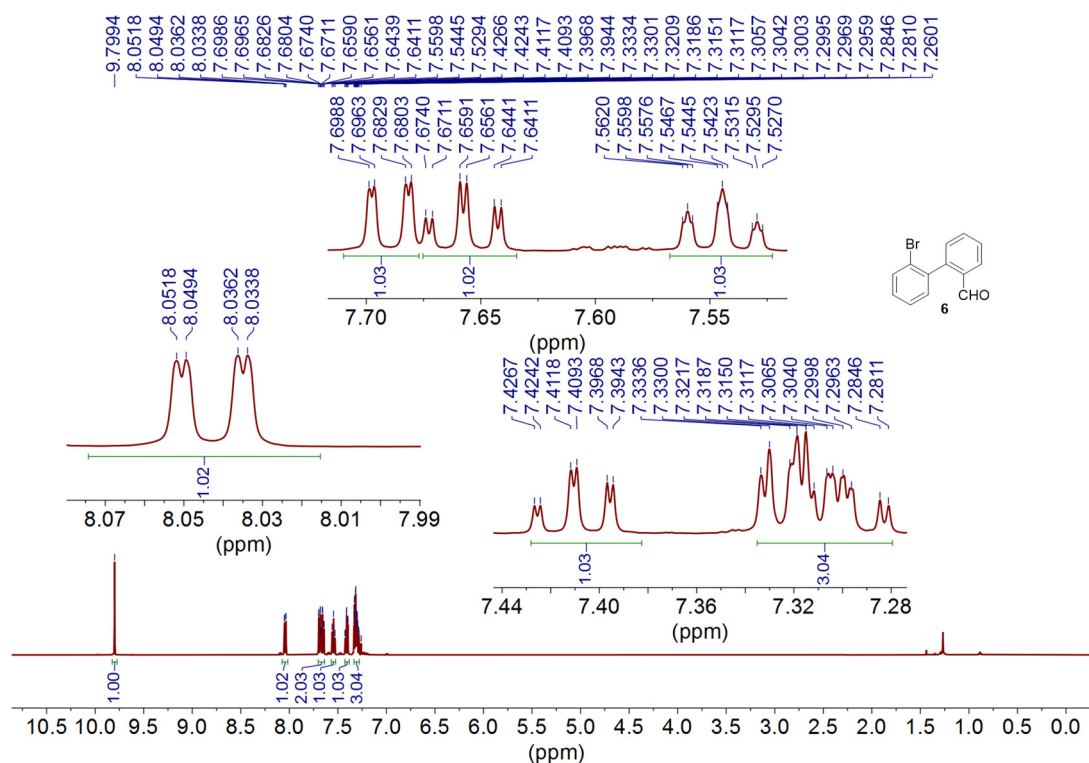
Figure S22. ^{1}H NMR (500 MHz) spectra of **6** recorded in CDCl$_3$ at room temperature.
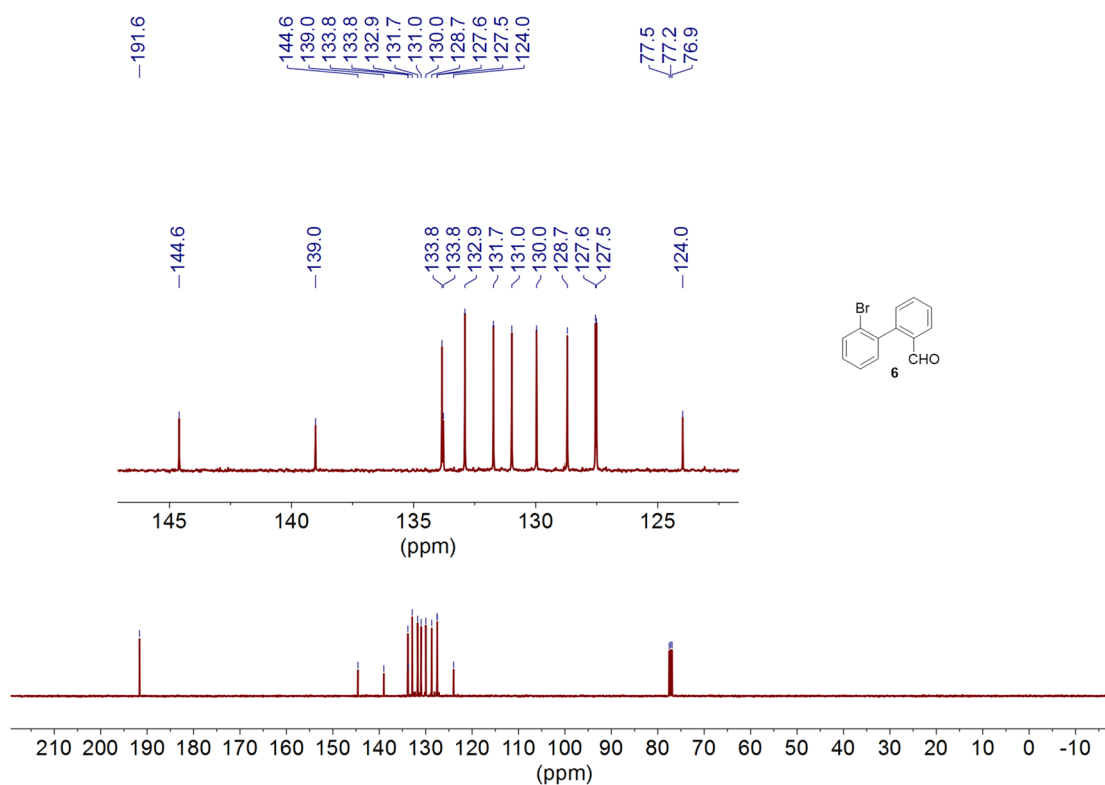
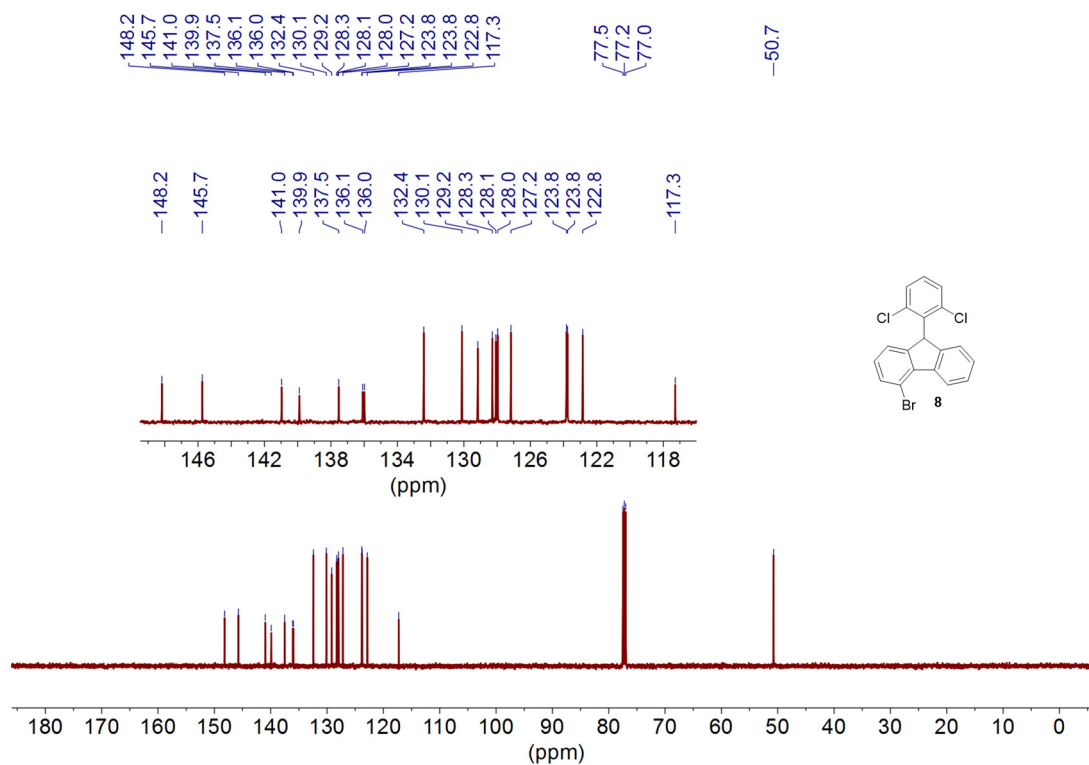**Figure S23.** ^{13}C NMR (125 MHz) spectra of **6** recorded in CDCl$_3$ at room temperature.
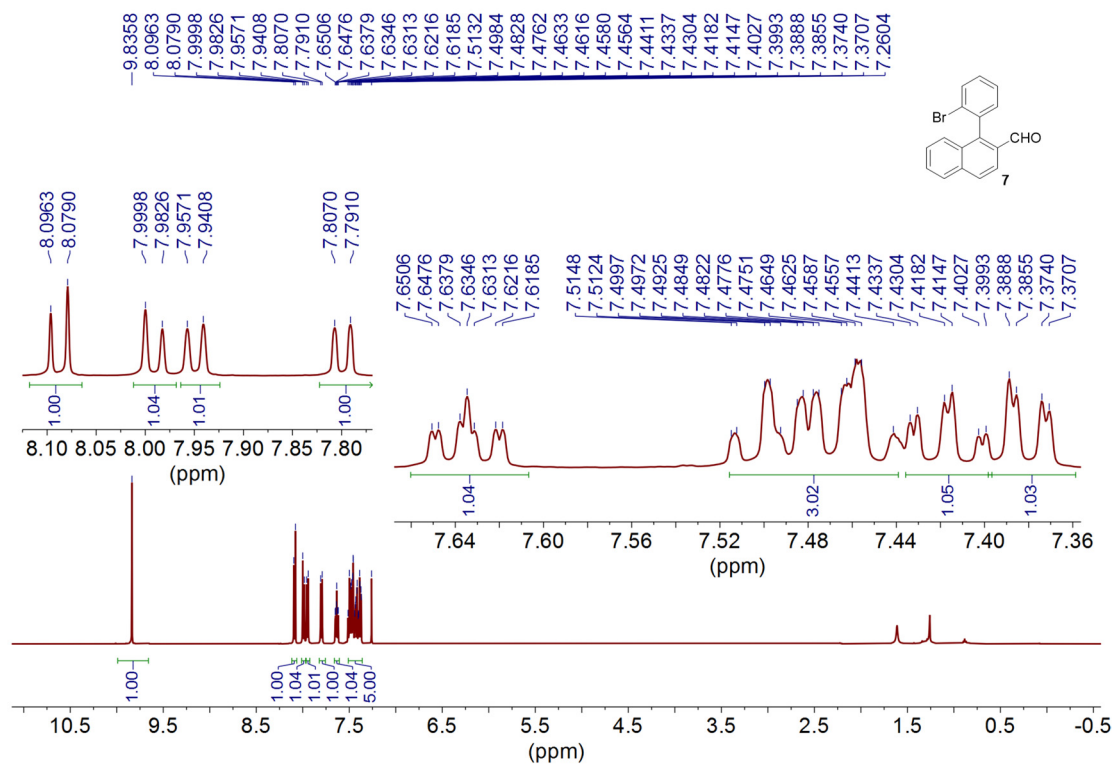
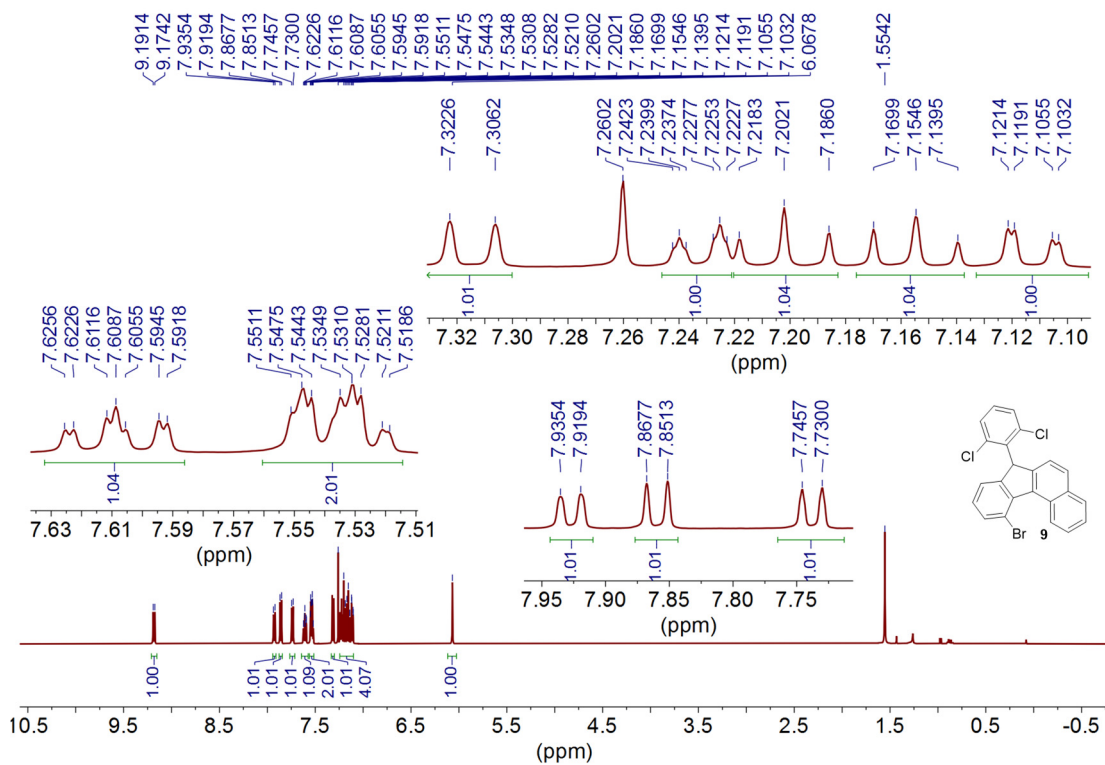**Figure S24.** ^{1}H NMR (500 MHz) spectra of **7** recorded in CDCl$_3$ at room temperature.
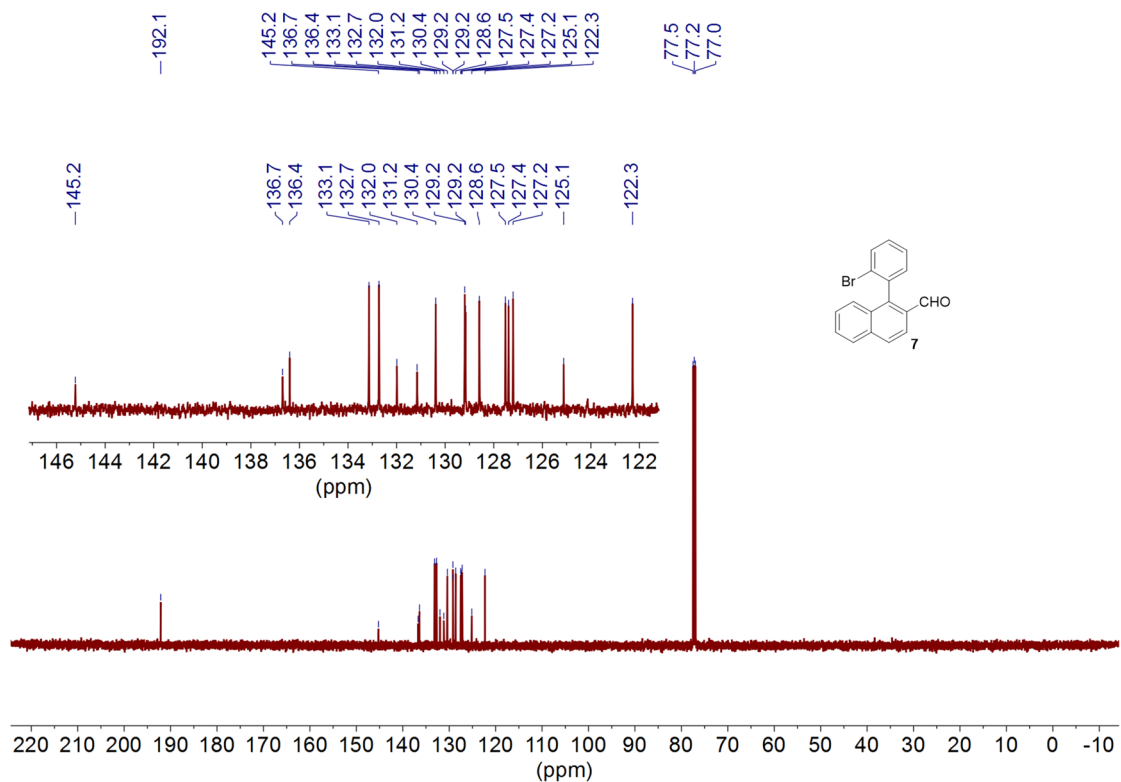
Figure S25. ^{13}C NMR (125 MHz) spectra of **7** recorded in CDCl$_3$ at room temperature.
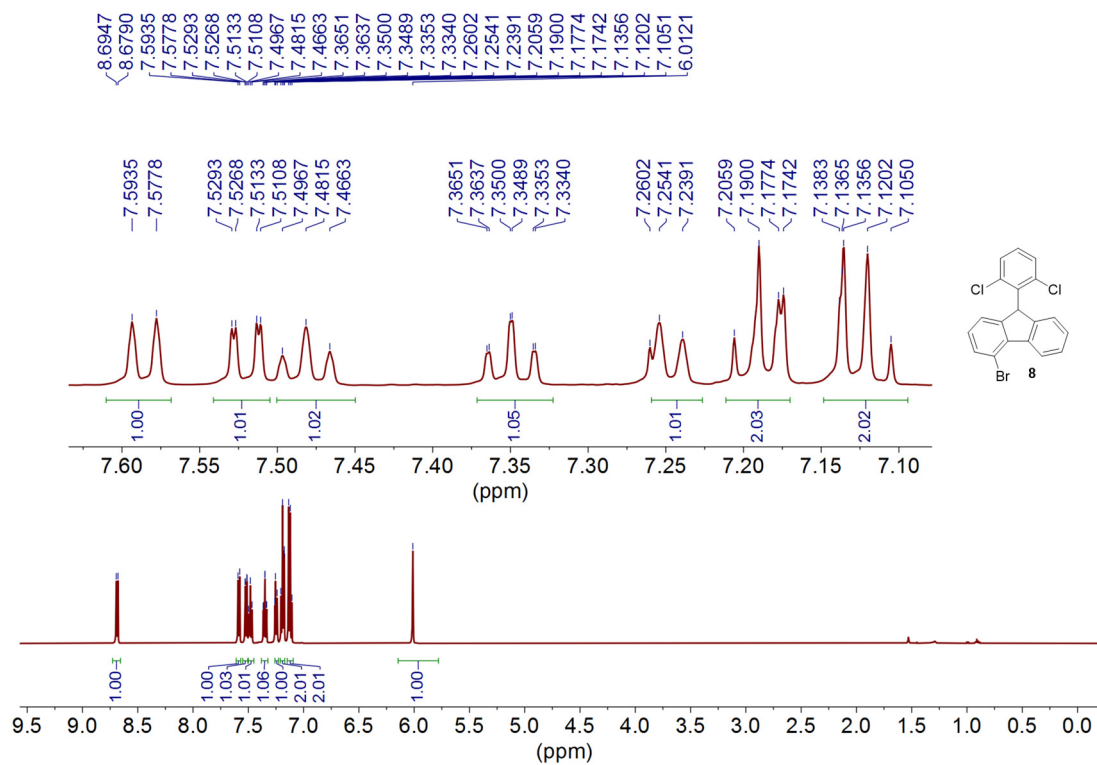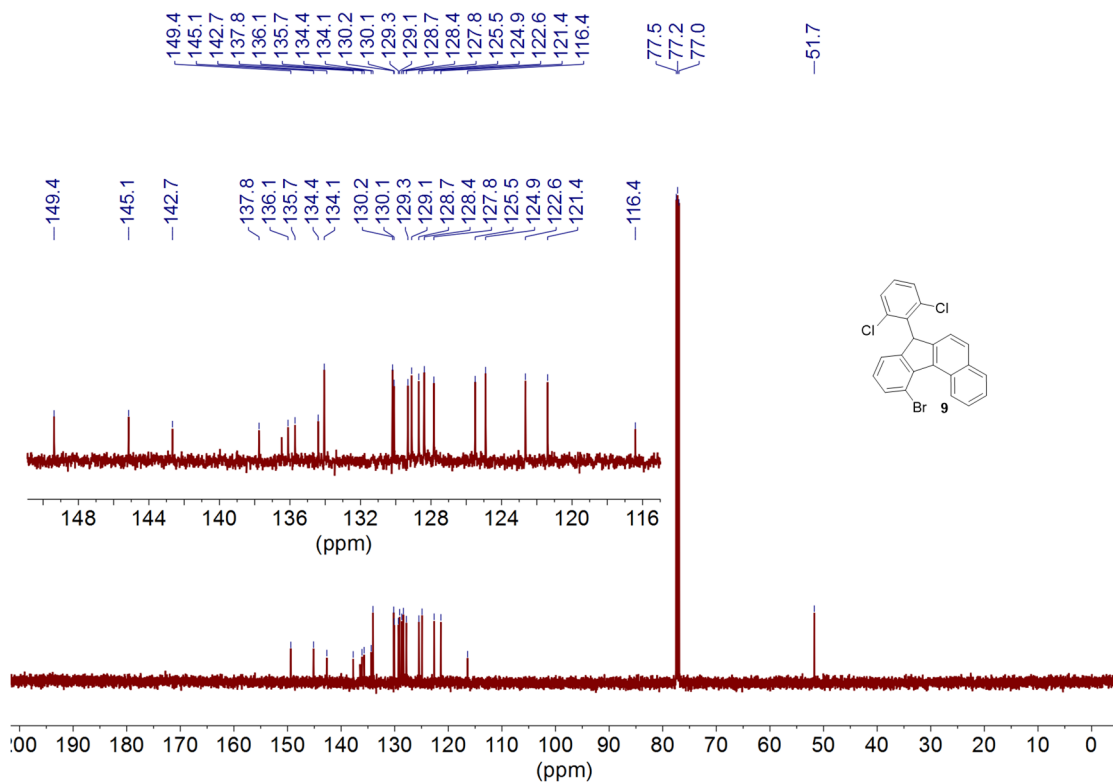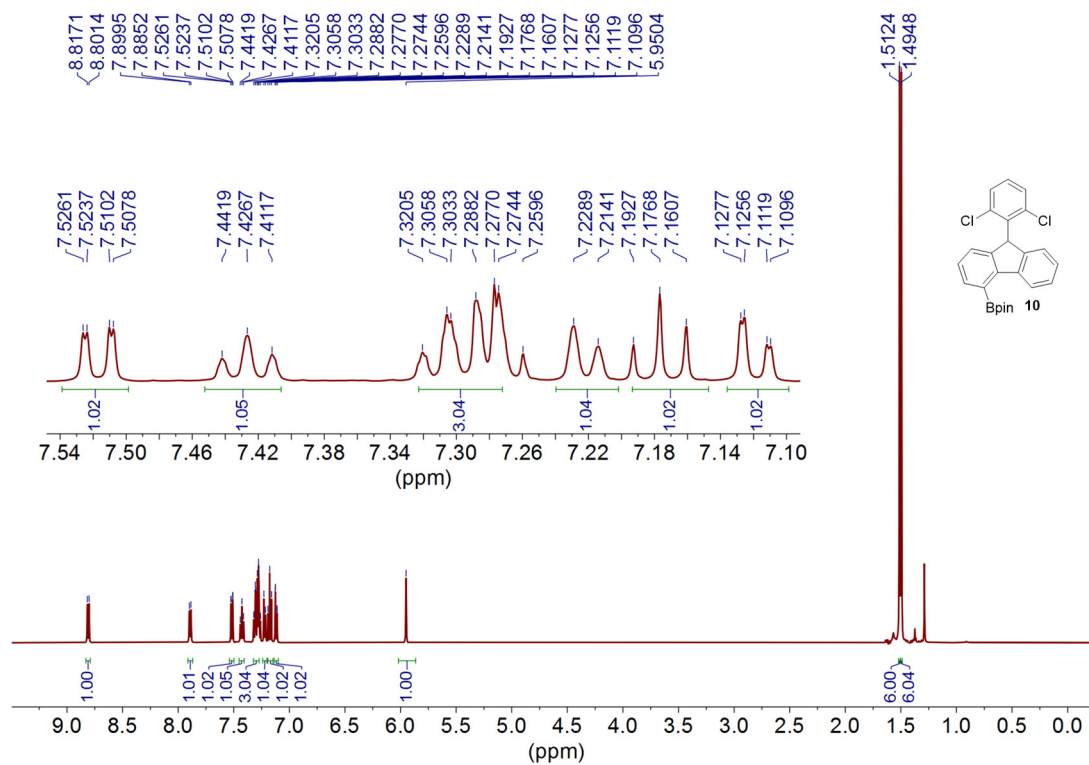
Figure S26. ^{1}H NMR (500 MHz) spectra of **8** recorded in CDCl$_3$ at room temperature.

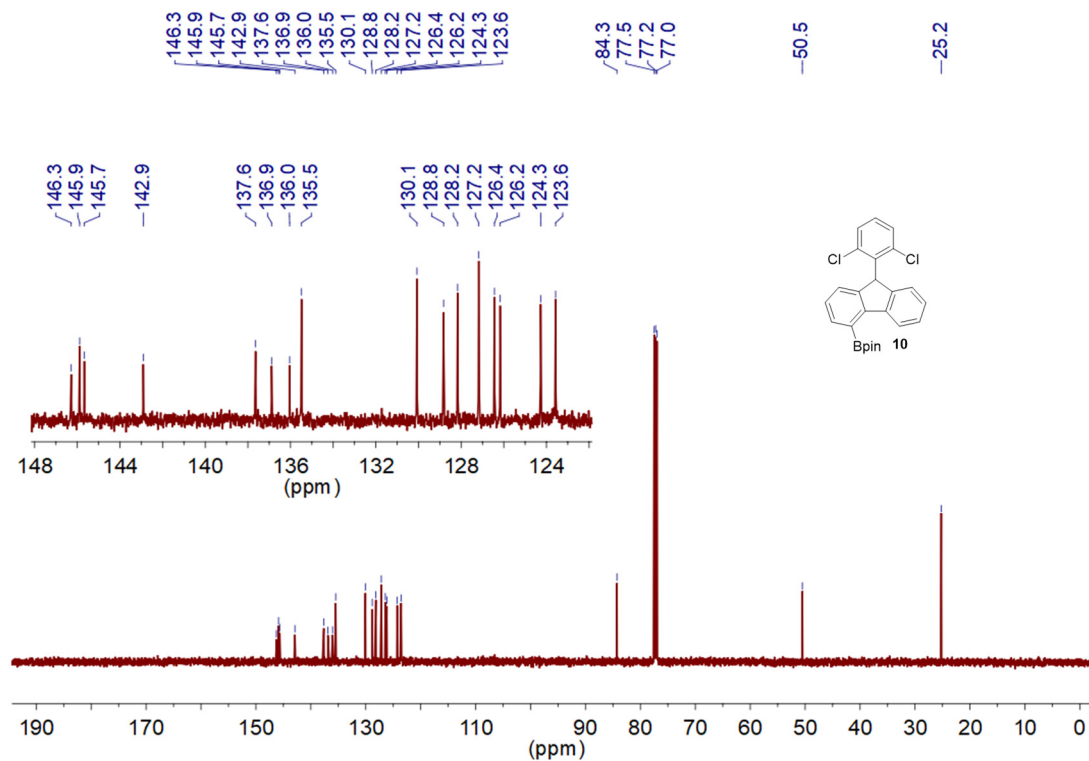**Figure S27.** ^{13}C NMR (125 MHz) spectra of **8** recorded in CDCl$_3$ at room temperature.

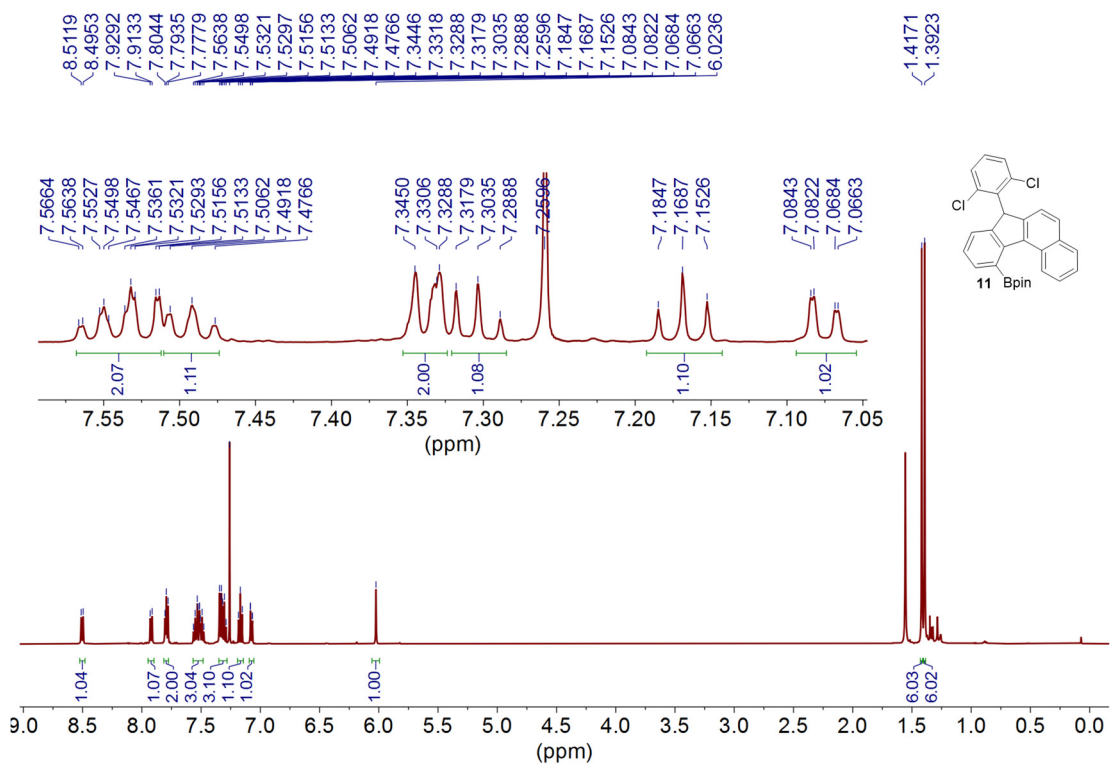**Figure S28.** ¹H NMR (500 MHz) spectra of **9** recorded in CDCl₃ at room temperature.

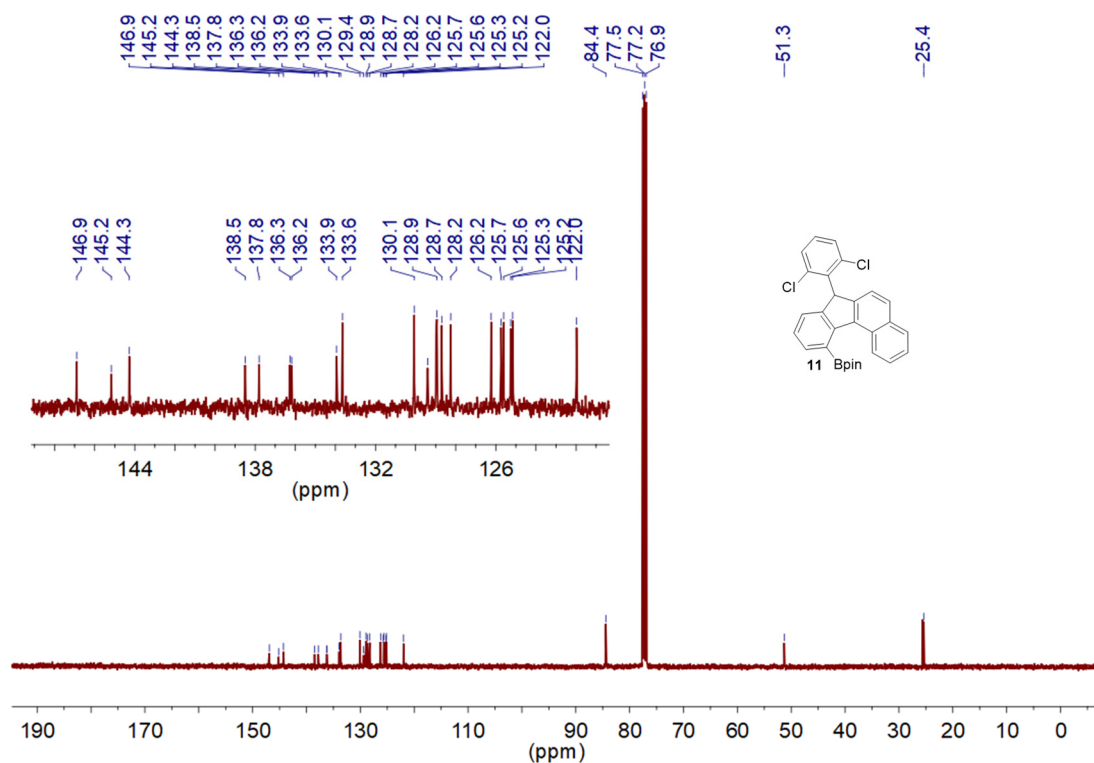**Figure S29.** ¹³C NMR (125 MHz) spectra of **9** recorded in CDCl₃ at room temperature.

Figure S30. ^{1}H NMR (500 MHz) spectra of **10** recorded in CDCl$_3$ at room temperature.
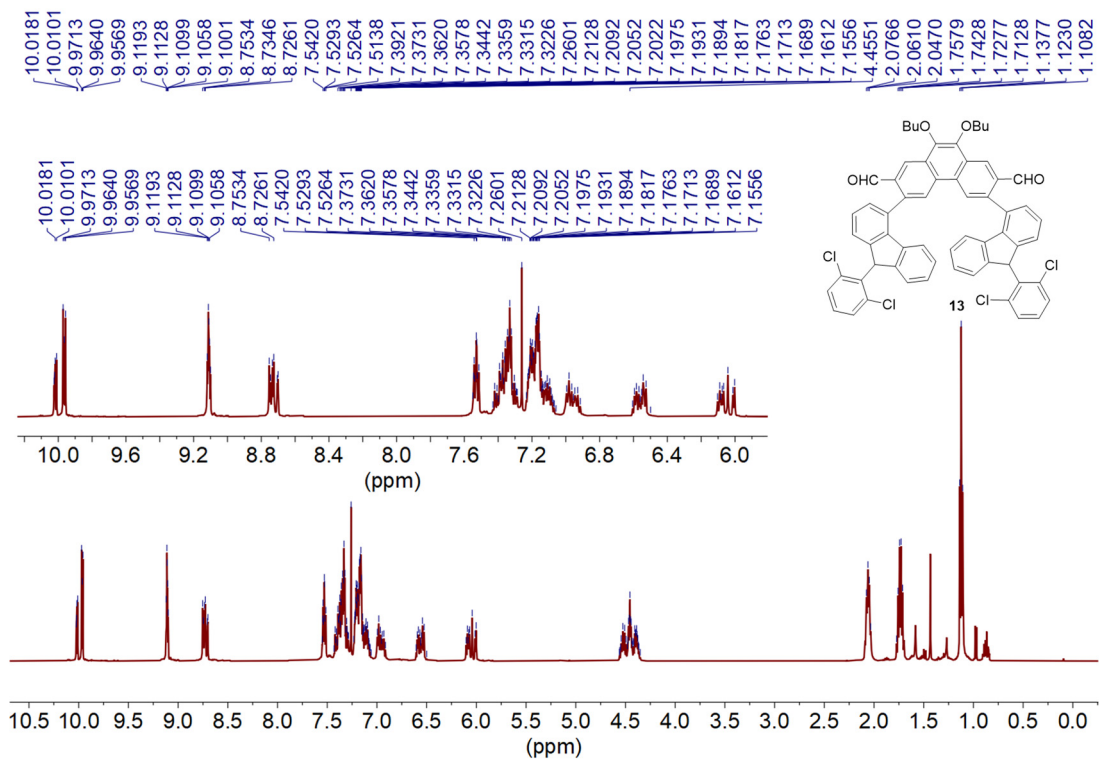

Figure S31. ^{13}C NMR (125 MHz) spectra of **10** recorded in CDCl$_3$ at room temperature.

Figure S32. ^{1}H NMR (500 MHz) spectra of **11** recorded in CDCl$_3$ at room temperature.

Figure S33. ^{13}C NMR (125 MHz) spectra of **11** recorded in CDCl$_3$ at room temperature.

Figure S34. ^{1}H NMR (500 MHz) spectra of **13** recorded in CDCl$_3$ at room temperature.

Figure S35. ^{13}C NMR (125 MHz) spectra of **13** recorded in CDCl$_3$ at room temperature.
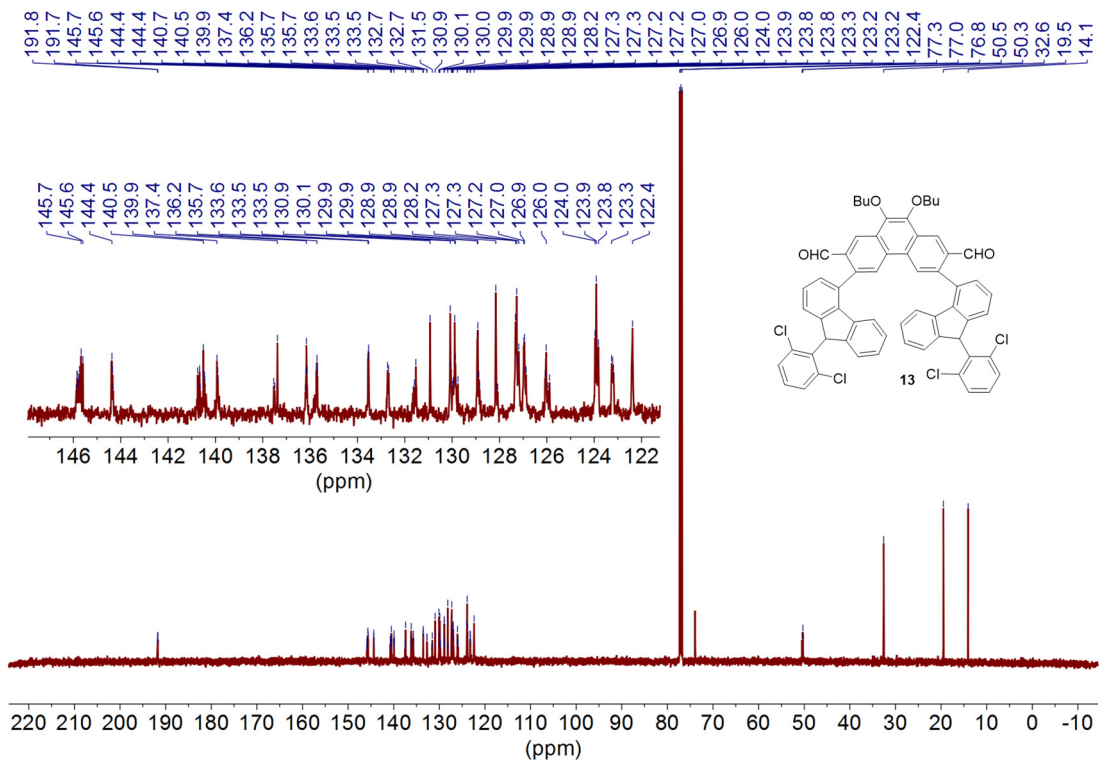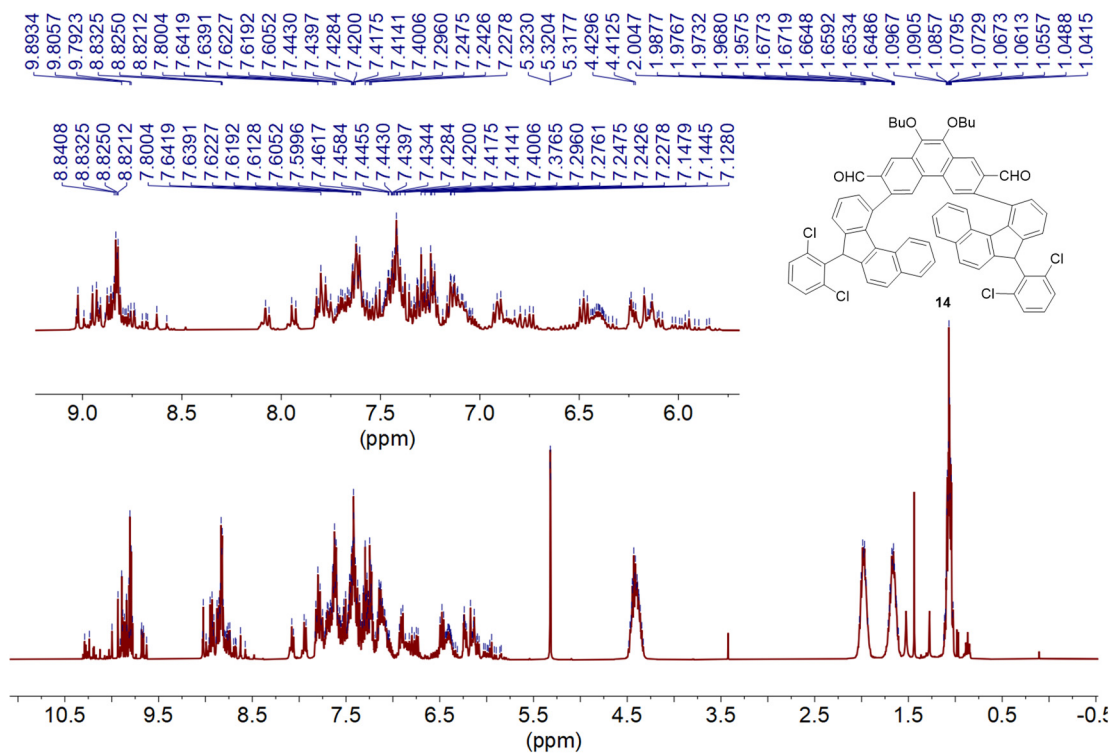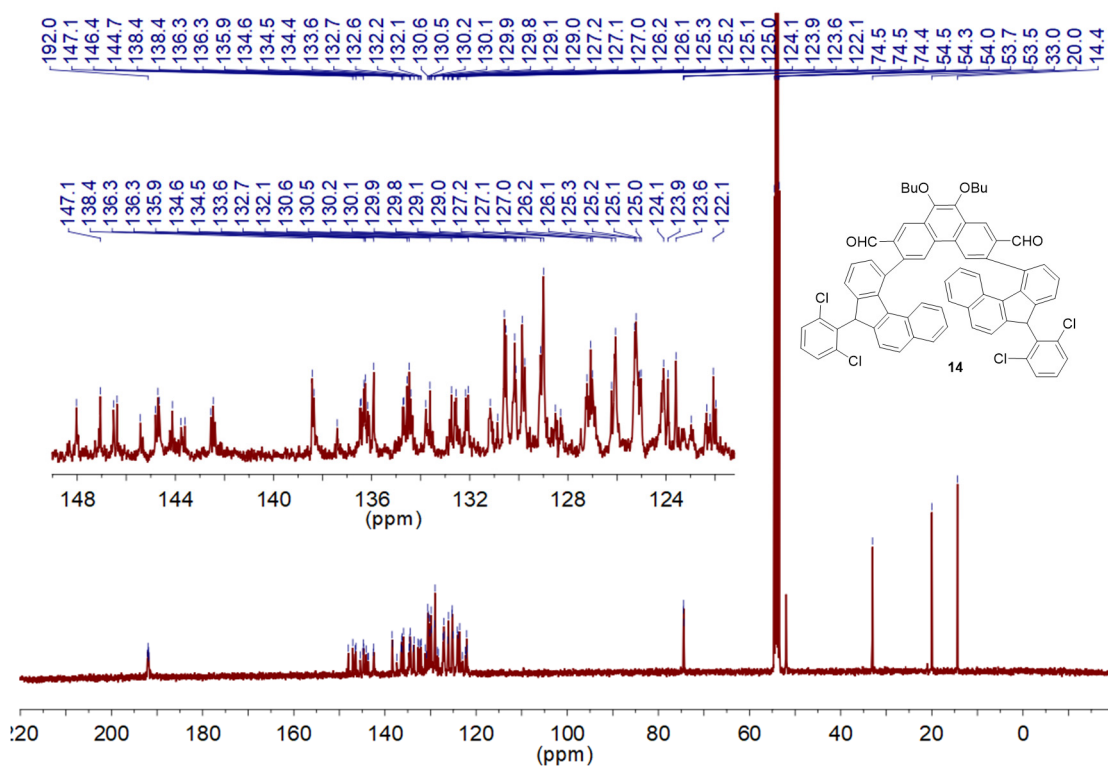
Figure S36. ^{1}H NMR (500 MHz) spectra of **14** recorded in CD$_2$Cl$_2$ at room temperature.

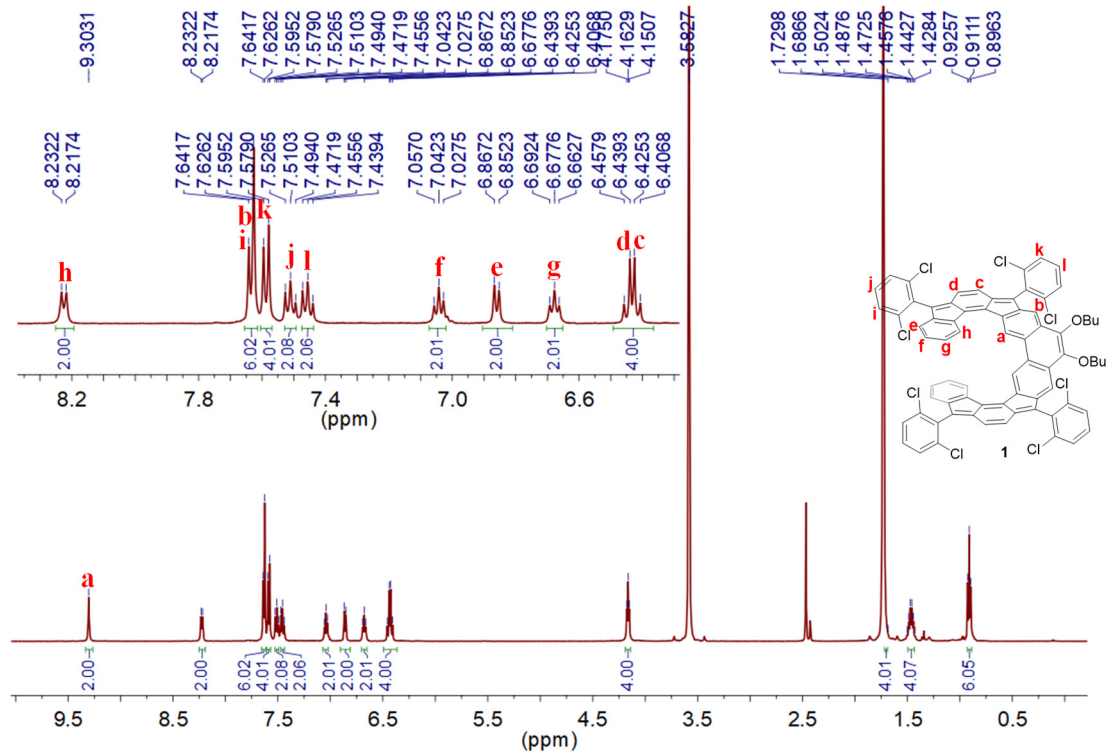**Figure S37.** ^{13}C NMR (125 MHz) spectra of **14** recorded in CD$_2$Cl$_2$ at room temperature.

Figure S38. ^{1}H NMR (500 MHz) spectra of **1** recorded in THF-d_8 at room temperature.

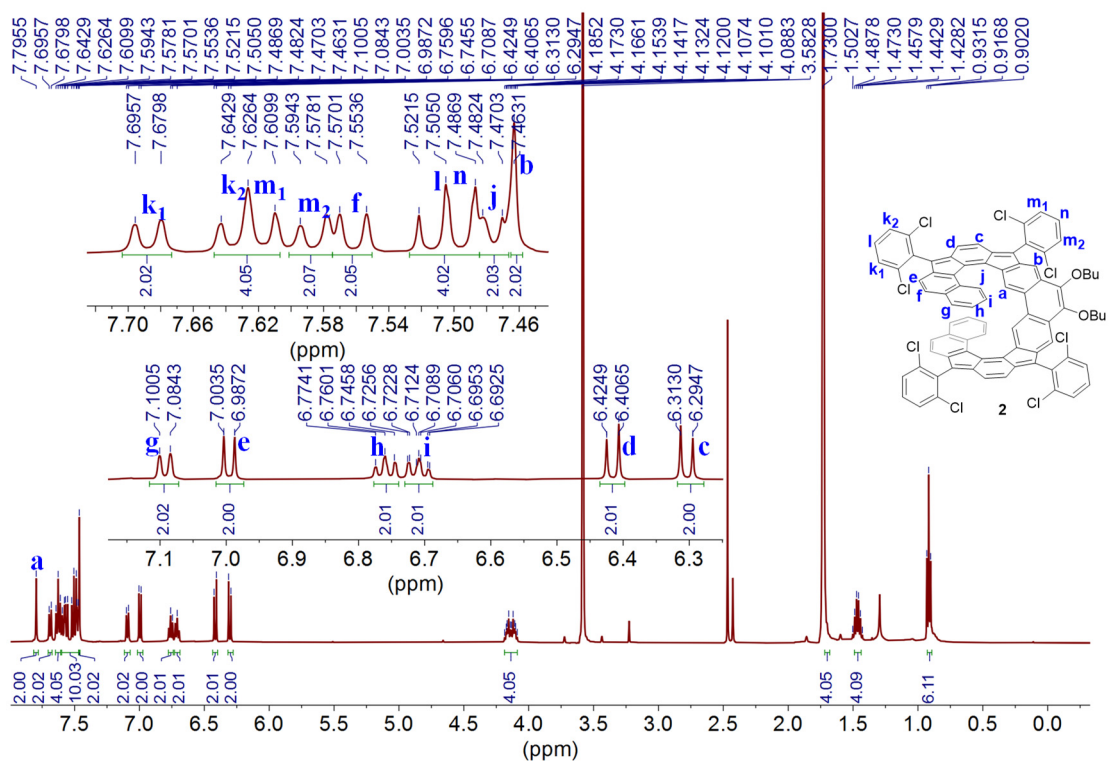**Figure S39.** ^{1}H NMR (500 MHz) spectra of **2** recorded in THF-d_8 at room temperature.

Mass Spectrum SmartFormula Report

Analysis Info   Acquisition Date   6/21/2019 3:19:13 PM

Analysis Name   D:\Data\Chem\2019 Samples\201906\0621\JQ-C1-1.d
Method   high mass-20181218.m   Operator   default user
Sample Name   JQ-P2   Instrument / Ser# micrOTOF-Q II 10269
Comment   A/P Chi Chunyan

Acquisition Parameter
Source Type   APCI   Ion Polarity   Positive   Set Nebulizer   3.0 Bar
Focus   Not active   Set Capillary   4500 V   Set Dry Heater   200 °C
Scan Begin   200 m/z   Set End Plate Offset -500 V   Set Dry Gas   4.0 l/min
Scan End   3000 m/z   Set Collision Cell RF 600.0 Vpp   Set Divert Valve   Waste

Meas. m/z	#	Formula	m/z	err [ppm]	rdb	e⁻ Conf	N-Rule
1247.1073	1	C 74 H 47 Cl 8 O 2	1247.1079	0.5	47.5	even	ok

Figure S40. High-resolution (HR) mass spectrum (APCI) of compound **1**.

Mass Spectrum SmartFormula Report

Analysis Info

Analysis Name   D:\Data\Chem\2019 Samples\201906\0621\JQ-C2.d
Method   high mass-20181218.m
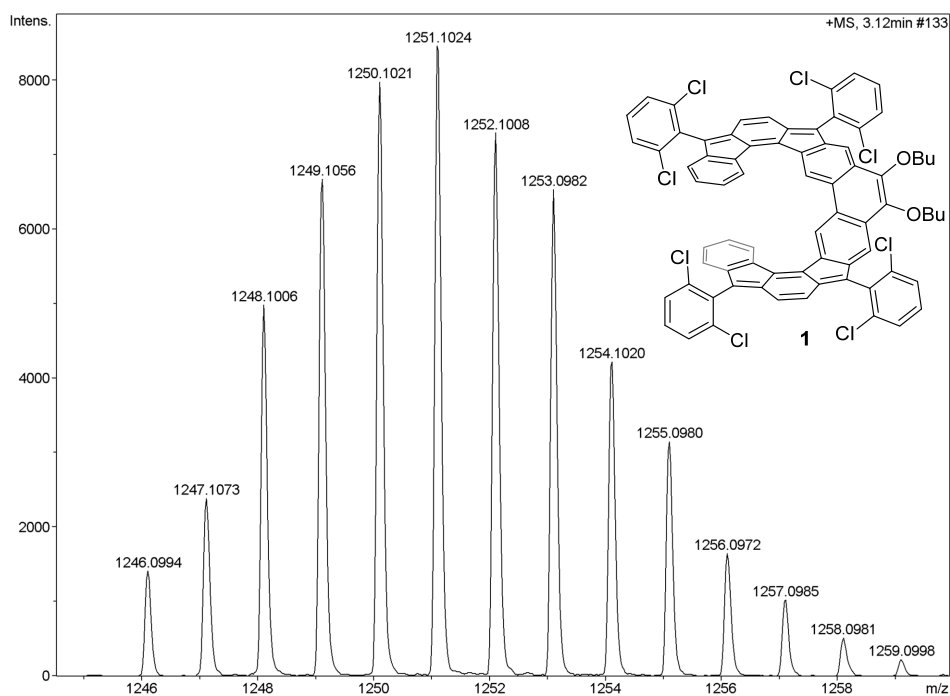Sample Name   JQ-C2
Comment   A/P Chi Chunyan

Acquisition Date   6/21/2019 3:35:06 PM
Operator   default user
Instrument / Ser#   micrOTOF-Q II 10269

Acquisition Parameter

Source Type	APCI	Ion Polarity	Positive	Set Nebulizer	3.0 Bar
Focus	Not active	Set Capillary	4500 V	Set Dry Heater	200 °C
Scan Begin	200 m/z	Set End Plate Offset	-500 V	Set Dry Gas	4.0 l/min
Scan End	3000 m/z	Set Collision Cell RF	600.0 Vpp	Set Divert Valve	Waste

Meas. m/z	#	Formula	m/z	err [ppm]	rdb	e⁻ Conf	N-Rule
1347.1369	1	C 82 H 51 Cl 8 O 2	1347.1392	1.7	53.5	even	ok
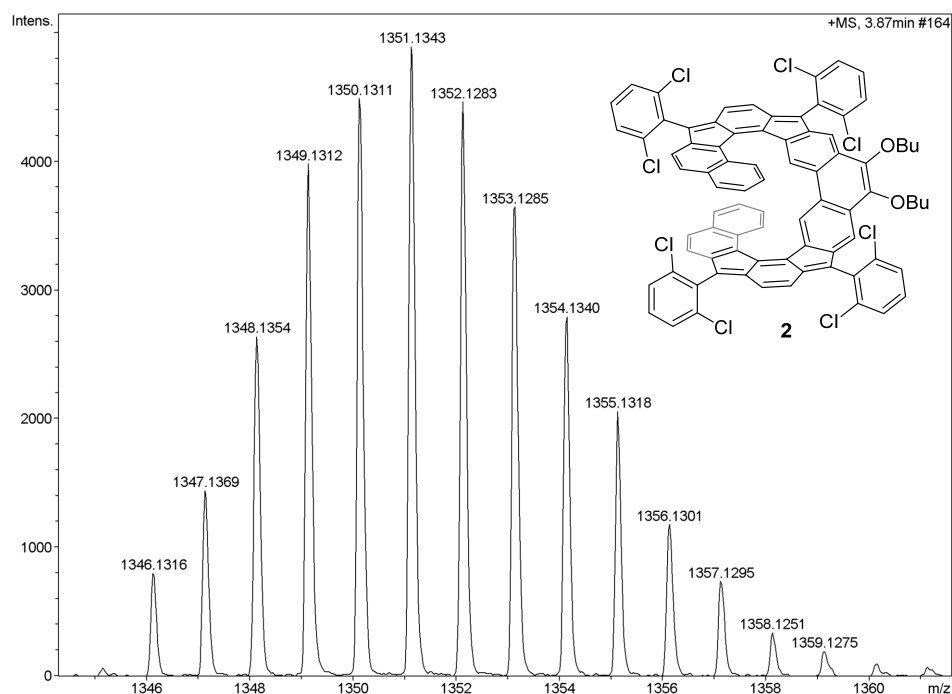
Bruker Compass DataAnalysis 4.0   printed: 6/21/2019 3:49:21 PM   Page 1 of 1

Figure S41. HR mass spectrum (APCI) of compound **2**.

6. References

(1) F. P. Gasparro, N. H. Kolodny, J. Chem. Educ. **1977**, 54, 258.

(2) *Gaussian 09; Revision D.01*; M. J. Frisch, G. W. Trucks, H. B. Schlegel, G. E. Scuseria, M. A. Robb, J. R. Cheeseman, G. Scalmani, V. Barone, B. Mennucci, G. A. Petersson, H. Nakatsuji, M. Caricato, X. Li, H. P. Hratchian, A. F. Izmaylov, J. Bloino, G. Zheng, J. L. Sonnenberg, M.

Hada, M. Ehara, K. Toyota, R. Fukuda, J. Hasegawa, M. Ishida, T. Nakajima, Y. Honda, O. Kitao, H. Nakai, T. Vreven, J. A. Montgomery, Jr., J. E. Peralta, F. Ogliaro, M. Bearpark, J. J. Heyd, E. Brothers, K. N. Kudin, V. N. Staroverov, R. Kobayashi, J. Normand, K. Raghavachari, A. Rendell, J. C. Burant, S. S. Iyengar, J. Tomasi, M. Cossi, N. Rega, J. M. Millam, M. Klene, J. E. Knox, J. B. Cross, V. Bakken, C. Adamo, J. Jaramillo, R. Gomperts, R. E. Stratmann, O. Yazyev, A. J. Austin, R. Cammi, C. Pomelli, J. W. Ochterski, R. L. Martin, K. Morokuma, V. G. Zakrzewski, G. A. Voth, P. Salvador, J. J. Dannenberg, S. Dapprich, A. D. Daniels, Ö. Farkas, J. B. Foresman, J. V. Ortiz, J. Cioslowski, and D. J. Fox, Gaussian, Inc., Wallingford CT, **2009**.

(3) (a) A. D. Becke, *J. Chem. Phys.* **1993**, *98*, 5648. (b) C. Lee, W. Yang, R. G. Parr, *Phys. Rev. B: Condens. Matter* **1988**, *37*, 785. (c) T. Yanai, D. Tew, N. Handy, *Chem. Phys. Lett.* **2004**, *393*, 51. (d) R. Ditchfield, W. J. Hehre, J. A. Pople, *J. Chem. Phys.* **1971**, *54*, 724. (e) W. J. Hehre, R. Ditchfield, J. A. Pople, *J. Chem. Phys.* **1972**, *56*, 2257. (f) P. C. Hariharan, J. A. Pople, *Theor. Chim. Acta* **1973**, *28*, 213.

(4) (a) S. Yamanaka, M. Okumura, M. Nakano and K. Yamaguchi, *J. Mol. Struct.* **1994**, *310*, 205. (b) K. Kamada, K. Ohta, A. Shimizu, T. Kubo, R. Kishi, H. Takahashi, E. Botek, B. Champagne and M. Nakano, *J. Phys. Chem. Lett.* **2010**, *1*, 937.

(5) (a) Z. Chen, C. S. Wannere, C. Corminboeuf, R. Puchta, P. v. R. Schleyer, *Chem. Rev.* **2015**, *105*, 3842. (b) H. Fallah-Bagher-Shaidaei, S. S. Wannere, C. Corminboeuf, R., Puchta, P. v. R. Schleyer, *Org. Lett.* **2006**, *8*, 863.

(6) D. Geuenich, K. Hess, F. Köhler, R. Herges, *Chem. Rev.* **2005**, *105*, 3758.

(7) (a) C. Gonzalez, H. B. Schlegel, *J. Chem. Phys.* **1989**, 90, 2154. (b) C. Gonzalez, H. B. Schlegel, *J. Phys. Chem.* **1990**, 94, 5523.